TROPICAL SYNOPTIC SCALE MOISTURE FIELDS

OBSERVED FROM THE NIMBUS–7 SMMR

A Thesis

by

JEFFREY DAVID FINK

Submitted to the Office of Graduate Studies of
Texas A&M University
in partial fulfillment of the requirements for the degree of

MASTER OF SCIENCE

May 1989

Major Subject: Meteorology

REPORT DOCUMENTATION PAGE

Form Approved
OMB No. 0704-0188

1a. REPORT SECURITY CLASSIFICATION UNCLASSIFIED	1b. RESTRICTIVE MARKINGS NONE
2a. SECURITY CLASSIFICATION AUTHORITY	3. DISTRIBUTION/AVAILABILITY OF REPORT APPROVED FOR PUBLIC RELEASE; DISTRIBUTION UNLIMITED.
2b. DECLASSIFICATION/DOWNGRADING SCHEDULE	

4. PERFORMING ORGANIZATION REPORT NUMBER(S)	5. MONITORING ORGANIZATION REPORT NUMBER(S) AFIT/CI/CIA- 89-056

6a. NAME OF PERFORMING ORGANIZATION AFIT STUDENT AT TEXAS A&M UNIVERSITY	6b. OFFICE SYMBOL (If applicable)	7a. NAME OF MONITORING ORGANIZATION AFIT/CIA
6c. ADDRESS (City, State, and ZIP Code)		7b. ADDRESS (City, State, and ZIP Code) Wright-Patterson AFB OH 45433-6583

8a. NAME OF FUNDING/SPONSORING ORGANIZATION	8b. OFFICE SYMBOL (If applicable)	9. PROCUREMENT INSTRUMENT IDENTIFICATION NUMBER

8c. ADDRESS (City, State, and ZIP Code)	10. SOURCE OF FUNDING NUMBERS			
	PROGRAM ELEMENT NO.	PROJECT NO.	TASK NO	WORK UNIT ACCESSION NO.

11. TITLE (Include Security Classification) (UNCLASSIFIED)
Tropical Synoptic Scale Moisture Fields Observed from the NIMBUS-7 SMMR

12. PERSONAL AUTHOR(S)
Jeffrey David Fink

13a. TYPE OF REPORT THESIS/~~DISSERTATION~~	13b. TIME COVERED FROM _____ TO _____	14. DATE OF REPORT (Year, Month, Day) 1989 May	15. PAGE COUNT 71

16. SUPPLEMENTARY NOTATION
APPROVED FOR PUBLIC RELEASE IAW AFR 190-1
ERNEST A. HAYGOOD, 1st Lt, USAF
Executive Officer, Civilian Institution Programs

17.	COSATI CODES		18. SUBJECT TERMS (Continue on reverse if necessary and identify by block number)
FIELD	GROUP	SUB-GROUP	

19. ABSTRACT (Continue on reverse if necessary and identify by block number)

20. DISTRIBUTION/AVAILABILITY OF ABSTRACT ☒ UNCLASSIFIED/UNLIMITED ☐ SAME AS RPT. ☐ DTIC USERS	21. ABSTRACT SECURITY CLASSIFICATION UNCLASSIFIED
22a. NAME OF RESPONSIBLE INDIVIDUAL ERNEST A. HAYGOOD, 1st Lt, USAF	22b. TELEPHONE (Include Area Code) (513) 255-2259 22c. OFFICE SYMBOL AFIT/CI

DD Form 1473, JUN 86   Previous editions are obsolete.   SECURITY CLASSIFICATION OF THIS PAGE

AFIT/CI "OVERPRINT"

ABSTRACT

Tropical Synoptic Scale Moisture Fields Observed

from the NIMBUS-7 SMMR. (May 1989)

Jeffrey David Fink, B.S., Texas A&M University

Chair of Advisory Committee: Dr. James P. McGuirk

Nimbus-7 SMMR brightness temperatures from 7 days in January 1979 and 3 days in May 1979 are used to estimate precipitable water and precipitation over the tropical eastern Pacific Ocean. These estimates are made from algorithms developed by Wilheit and Chang (1980) for precipitable water and by Katsaros and Lewis (1986) and Lipes (1981) for precipitation. The SMMR estimates are compared with moisture estimates from TIROS-N infrared moisture channels, TIROS-N outgoing longwave radiation, and the ECMWF model analysis. Comparisons are made within the context of five typical tropical synoptic scale features: Tropical plumes (TP) synoptic scale disturbances viewed in the cloud field, linking the tropics and midlatitudes; the Subtropical High (STH), the dry region extending along the northwest flank of a TP; the active Intertropical Convergence Zone (AITCZ), banded equatorial convection over the eastern Pacific Ocean; the quiescent Intertropical Convergence Zone (QITCZ), areas with no convective cloud tops present along the ITCZ; and the Equatorial Dry Zone (EDZ), an area along and south of the equator between 100°W and 120°W.

SMMR precipitable water estimates provide detailed information on the moisture structure in all areas of the tropics except in areas of heavy precipitation.

Most of the information present in the TIROS-N and ECMWF data identifies the synoptic feature and not variations within a feature. SMMR data identified TP precipitable water content as statistically identical to a QITCZ and the precipitation as statistically identical to AITCZ precipitation. Prediction of SMMR precipitable water using TIROS-N and ECMWF data explained 67% of the variance in SMMR data while ECMWF analysis alone explained 55% of the variance.

Accesion For	
NTIS CRA&I	☑
DTIC TAB	☐
Unannounced	☐
Justification	
By	
Distribution /	
Availability Codes	
Dist	Avail and / or Special
A-1	

ACKNOWLEDGMENTS

TABLE OF CONTENTS

LIST OF TABLES

LIST OF FIGURES

CHAPTER I

INTRODUCTION

Synoptic features of the equatorial eastern Pacific Ocean weather systems are easy to observe on visual and infrared satellite images. However, it is difficult to quantify their moisture fields due to the great scarcity of conventional data. In addition, it is difficult to examine rainfall over the eastern part of the tropical Pacific Ocean because there are few island stations or ship reports available.

Satellite passive microwave instruments have been used to determine precipitable water, liquid water and precipitation over oceans. Passive microwave sensors detect moisture in the atmosphere over oceans by modification of the relatively uniform brightness temperature of the ocean surface in the presence of water vapor, liquid water and precipitation.

In this study Nimbus-7 Scanning Multichannel Microwave Radiometer (SMMR) derived precipitable water and precipitation estimates, TIROS-N Operational Vertical Sounder Channel 11 and 12 (TOVS 11 and TOVS 12) brightness temperatures, outgoing longwave radiation (OLR) data, and GOES infrared (IR) imagery are used to investigate moisture content and precipitation over the tropical Pacific Ocean. The data are compared within the context of five typical tropical features: the Tropical Plume (TP), a synoptic cloud disturbance linking the tropics and midlatitudes; the Subtropical High (STH), the dry region extending along the northwest flank of a

---

The style is similar to that of the *Journal of the Atmospheric Sciences.*

TP; the Active ITCZ (AITCZ), banded equatorial convection over the eastern Pacific Ocean; the Quiescent ITCZ (QITCZ), areas of the ITCZ where no convective cloud tops are present; the Equatorial Dry Zone (EDZ), an area of subsidence along and south of the equator between $90°$ and $120°$ W.

Quantitative comparisons are made by statistical correlation, examination of means and standard deviations and multiple regression. The results show differences in tropical features and capabilities of satellites to estimate precipitable water and precipitation over the tropical oceans.

A survey of previous work on the tropical Pacific Ocean and capabilities of satellite moisture data is presented in Chapter II. Chapter III defines the problem, establishes research objectives, and outlines research methodology. The SMMR, TOVS, ECMWF and OLR data sets are described in Chapter IV, along with the method of data collection. In Chapter V the precipitable water content of tropical features and precipitable water data is discussed. In Chapter VI the characteristics of rainfall from SMMR are discussed. A summary and discussion of results are presented in Chapter VII.

CHAPTER II

PREVIOUS WORK

The first satellite-borne passive microwave radiometer flew on the Cosmos-243, launched in 1968. The passive microwave data was used to estimate surface temperature, integrated water vapor content and cloud liquid water content. Subsequent satellites have had better resolution, greater accuracy and increased scan area.

The Nimbus-7 research satellite was in operational orbit from 1978-1987 with a SMMR instrument onboard. The sun–synchronous orbit provided twice daily coverage with local equator crossing times of noon and midnight. Due to power limitations on the satellite the SMMR duty cycle was limited to every other day. The instrument operated at 6.6, 10.7, 18, 21, and 36 GHz in both horizontal and vertical polarizations. A conical scan with a 50° incidence angle provided uniform footprint size in a swath of observations 780 km wide perpendicular to the suborbital track. Brightness temperatures observed by SMMR provide a unique opportunity to implement algorithms and retrieve geophysical parameters over the oceans. Gloersen et al. (1984) demonstrated that SMMR analyzed brightness temperatures provide good sea surface temperatures estimates, near surface winds, atmospheric precipitable water and rainfall rates over open oceans.

The atmospheric parameters available from SMMR are precipitable water, liquid water and rainfall. Wilheit and Chang (1980) developed an algorithm for the retrieval of these parameters. They showed that precipitable water can be accurately derived while rainfall and liquid water information are available in a somewhat limited

form. The algorithms use the modification of ocean surface brightness temperature in the different microwave frequencies by water vapor, liquid water and precipitation to estimate the amount of these quantities in the atmosphere. Prabhakara et al. (1982) demonstrated that precipitable water retrievals did not suffer from noise introduced by variations in sea surface temperature, surface wind, or liquid water content in non-raining clouds. Their comparisons of SMMR precipitable water estimates with coincident ship radiosondes showed a square root of the mean square error (rms) deviation from radiosondes of only about 2.5 kg m^{-2}. Spencer (1986), in a case study of convection over the Gulf of Mexico, developed an algorithm that used SMMR 37 GHz brightness temperature to estimate rainfall. Computed rainfall rates correlated well with radar estimated rainfall in his limited case study.

In a case study of North Pacific Ocean wintertime weather systems Katsaros and Lewis (1986) used Nimbus-7 SMMR to examine mesoscale and synoptic scale features. Their investigation of precipitable water and rainfall revealed features such as frontal undulations and rain cells under cirrus shields, even when these features approached the limit of sensor resolution. Rainfall estimates from a SMMR algorithm were compared to rainfall data at a coastal rain gauge network and found to be in reasonably good agreement.

Warner (1984) examined a summer monsoon depression in the Bay of Bengal using satellite and research aircraft data. Starting with published results gathered from research aircraft dropwindsondes and airborne radar, he added satellite data from the Microwave Sounding Unit (MSU) aboard TIROS-N and SMMR from Nimbus-7 to enhance the analysis. Estimations of precipitable water amounts obtained from

SMMR were found to be in good agreement with those from dropsondes. SMMR inferred rainfall amounts were less accurate when compared to estimates from airborne radar, but the percentages of area covered by rain were similar in the two methods. Due to the inadequate coverage in time and space of the experimental satellite data Warner was unable to develop a comprehensive description of a monsoon depression using only satellite data.

McGuirk and Thompson (1984) in an investigation of the tropical eastern Pacific Ocean defined TPs as characterized by a continuous band of upper and mid-level clouds at least 2000 km long originating close to the equator and extending north of 15° N. Using First GARP Global Experiment (FGGE) IIIb moisture analyses. Schaefer (1985) made observations about the two January TPs used in this case study. He observed the moisture field was at least partially unconnected to the ITCZ and that TPs results from a combination of interrelated elements. Stockton (1986), in another TP case study, used TOVS 11 and TOVS 12 channel moisture data. He observed that the moisture field of a TP appeared strongest in the channel 12 signal, which has a weighting function centered near 500 mb. Stockton also developed a model describing the conditions accompanying TP development. Two of the conditions he identified were a low level moisture source and enhanced convection in the ITCZ, both of these conditions can be detected by SMMR data. McGuirk et al. (1987) suggested two possible subclasses of TP: those originating from cold-frontal cloud bands and those that originate near the ITCZ. These two different origins might imply different spatial distributions of moisture that could be detected by SMMR.

Hayes (1988) investigated the cool season Pacific Ocean ITCZ in an eight year period of OLR data prepared by the National Oceanic and Atmospheric Administration (NOAA). Hayes identified active and quiescent periods of convection using OLR data and described the movement and variability of these periods. He found that the position of maximum convection shifts quickly, moving up to 15° latitude over a few days. The ITCZ active convection also moves south when TPs are present. The movement of convection will separate the TP and ITCZ precipitation.

Anderson (1986) examined the information content of the TOVS full channel soundings over the tropical Pacific Ocean. His investigation found the TOVS channels will vary according to the synoptic condition and are sensitive to water vapor and cloud amount. Attempts to augment TOVS in cloudy regions were only partially successful, so the TOVS data does not reflect the actual conditions in cloudy regions. His methodology was found to augment synoptic analysis in this data sparse region.

McGuirk et al. (1989) examined the capabilities and limitations of five synoptic scale moisture observing systems in the tropical Pacific Ocean: surface observations, satellite cloud imagery, radio- and dropsondes, satellite individual channel brightness temperatures, and the European Center for Medium Range Weather Forecast (ECMWF) model moisture analysis. They performed both qualitative and quantitative intercomparisions to examine what the different observing system detect in the moisture field. Their investigation found that each observation type has its own strengths and weaknesses in detecting synoptic scale moisture and that each type of

data contains an independent signal. The satellite IR data was found to be a sensitive function of synoptic conditions. Their conclusion was that incorporating satellite data into the model analysis should result in an improved model analysis.

In summary, several studies have shown that SMMR can be used to estimate precipitable water and rainfall. Furthermore, other forms of satellite data have been used to measure moisture in the atmosphere. Therefore, it is justifiable to use satellite moisture estimates and the ECMWF model analysis of moisture to describe tropical synoptic moisture processes.

CHAPTER III

RESEARCH OBJECTIVES

The primary objective of this research is to describe quantitatively SMMR's capability to observe moist processes in synoptic features over the tropical Pacific Ocean and evaluate a method of reproducing SMMR precipitable water values. A crucial hypothesis is that, outside of heavy precipitation regions and over the open undisturbed ocean surface, SMMR represents an effective "ground truth" observation of atmospheric precipitable water content. No such ground truth exists for precipitation estimates since radar observation are absent over the eastern tropical Pacific Ocean. To fulfill this objective, several tasks were accomplished.

Estimate precipitable water from SMMR, TOVS 11, TOVS 12, OLR, and the ECMWF analysis.

Stratify the data by synoptic feature to reveal the behavior of the data and characteristics of the moisture fields within specific synoptic features.

Intercompare synoptic features using descriptive statistics to identify mean values and standard deviations of the moisture estimators.

Predict SMMR from alternate and more available TOVS 11, TOVS 12, OLR and ECMWF data sets.

Evaluate the precipitable water prediction scheme over the tropical Pacific Ocean within different synoptic features.

Estimate rainrates from SMMR within the TP and AITCZ (the only precipitating synoptic features in the study).

Evaluate and compare the frequency of rainrates within the TP and AITCZ and area coverage of precipitation within the TP.

CHAPTER IV

DATA

The data amassed for seven days in January and three days in May 1979 consist of conventional visible and IR satellite images, TOVS channel radiances, TIROS-N OLR, Nimbus-7 SMMR and the ECMWF model–generated moisture field. The data are used to identify features in the tropical Pacific Ocean from 30°N to 20°S and 180°–90°W. The TOVS 11, TOVS 12, OLR, and ECMWF data used in previous studies are combined to predict SMMR. Precipitation estimates within the features are done using SMMR data.

Discussion of data used in the estimation of moisture is presented first. Then the method of data sampling for the precipitable water analysis and prediction of SMMR precipitable water is explained. The algorithms used to process the SMMR data into rainrate estimates are presented with a discussion on the characteristics of the algorithms.

SMMR- CELL data tapes were processed using an algorithm presented in SASC (1985b), originally developed by Wilheit and Chang (1980) for use over the oceans. The CELL data are described in SASC (1985a) as satellite brightness temperatures that have been mapped into equal area, evenly-spaced, square cells across the swath of the SMMR scan. The cells are organized into blocks approximately 780 km cross–track by 788 km along–track. This study uses the 18, 21 and 37 GHz channels at a resolution of 60 km. Corrections applied to the CELL data

are presented by Gloersen (1987) for radiometric calibration, polarization mixing, sun shining in the cold horn, and beam spillover into space. Sun glint off the ocean surface was discussed by Beauchamp (1988), but is a problem only in specific areas of the southern hemisphere outside the study area. Additional problems involving erratic behavior of the brightness temperature calibration from July 1986 to December 1986 are discussed by Fu and Chung (1988) and long term drift of the 21 GHz horizontal polarization are discussed by Kim et al. (1984). The last two problems were avoided by selecting short time periods during the first year of SMMR operation.

An example of SMMR data are shown in Fig. 1. The figure has four consecutive SMMR orbits overlaid on a schematic of the GOES IR image. From left to right the SMMR orbit numbers and equator crossing times are 1302/1140 GMT (approximate observation time of the IR image), 1301/0955 GMT, 1300/0810 GMT and 1299/0630 GMT. SMMR data times correspond to a local midnight equator crossing time. The SMMR equator crossing times can differ from the standard data times of 00 GMT and 12 GMT by as much as five hours at 100°W. The SMMR observations are precipitable water estimates based on the brightness temperature of the 18 GHz and 21 GHz horizontal and vertical channels, processed through Wilheit and Chang (1980) algorithm.

The overall precipitable water pattern aligns well with the cloud features and provides a typical representation of the coverage SMMR data provides over the
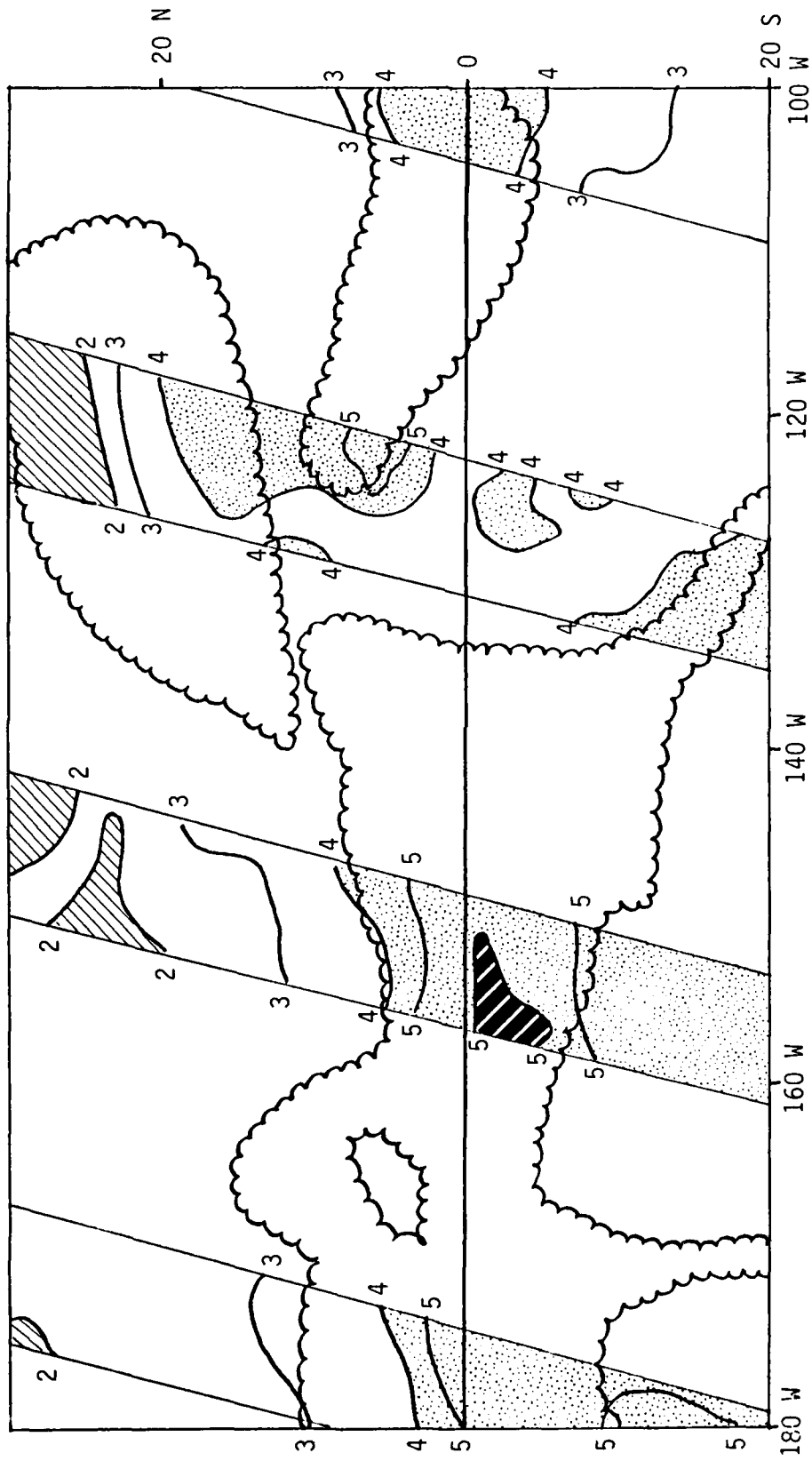
Figure 1. SMMR estimates of precipitable water (contoured in cm) from four consecutive SMMR passes. The SMMR passes are overlaid on a schematic of the 12 GMT GOES IR image for January 26, 1979. Stippling is moist; hatching is dry; dark hatching is contaminated by heavy precipitation; scalloped regions demarcate cloudy areas.

tropical Pacific Ocean. Evident in the figure are the high precipitable water content (greater then 5 cm) in the south Pacific convergence zone at 180°W and south of the equator. The precipitable water content is also high north of the equator in the ITCZ at 125°W. Contaminated estimates of precipit .... water south of the equator at 160°W are a result of heavy precipitation. Precipitation in SMMR orbit 1301 is estimated using an algorithm developed by Lipes (1981). The precipitation is in the ITCZ with the highest estimated rainrate of 9 mm h^{-1} and covers approximately 2460 km^2. The TP centered at 20°N and 130°W, although cloudy on the northwest edge has a relatively low precipitable water content. Low precipitable water values on the northwest border of TPs increasing to higher precipitable water values on the southern border of TPs are a common feature of TPs. Lack of precise agreement between the SMMR precipitable water estimates and cloud field at 120°W just north of the equator is due probably to the time differences of about 4 hours between the GOES image and the SMMR data.

TOVS 7.3 and 6.7 micrometer moisture channels, TOVS 11 and TOVS 12 respectively, from the TIROS–N satellite are gridded and analyzed at 250 km resolution and available on maps at 00 GMT and 12 GMT. Anderson (1986) processed the data tapes that used methods developed by Smith et al. (1979) to process the satellite radiances. A continuous map of the channel brightness temperatures over the entire domain was used for selection of the data.

OLR data are from the TIROS–N 10.5-12.5 micrometer IR window channel. The data are spatially averaged, digitized, and gridded at a 2.5° resolution. The

data tapes were processed by Hayes (1988) for 00 GMT and 12 GMT. Missing grid-points were filled by temporally averaging to 24 hour resolution and interpolating over adjacent space and time.

The ECMWF operational analysis/forecast model analysis of relative humidity estimates was used to calculate precipitable water. The analysis uses no satellite moisture data and can be considered independent of the other moisture estimates. The data were prepared previously and available on maps at 00 GMT and 12 GMT.

A set of collocated observations are taken to study means and standard deviations within different features and correlations between the data. First the GOES-West IR satellite image was used to identify five typical synoptic features. Then a set of collocated observations from all data types was taken to examine the relationships between different tropical features. To select the collocated observations one block of SMMR data (SMMR data has the most restrictive format) within each feature's boundaries was found for 00 GMT and 12 GMT. Then to maximize the number of observations nine evenly spaced observations from all data sets were selected. Sixty blocks of SMMR data are used in the data set with nine observations per block resulting in 540 collocated observations of SMMR, TOVS 11, TOVS 12, OLR and ECMWF. The observations are not all independent since the data are known to have spatial correlation. Anderson (1986) found the distance between uncorrelated data to vary from 700 km in the STH to 1500 km in the ITCZ. Using the rigorous definition of spatial independence would result in one observation from each of the 60 blocks being independent. The standard error (one standard deviation) of

the correlation coefficients assuming 60 independent observations is approximately r=0.3.

Each feature was identified descriptively from GOES IR imagery, as shown in Fig. 2. TP observations were selected from any portion of the TP north of 10°N in the central area of the TP avoiding the downwind thin and broken cirrus blowoff; the TP was defined by McGuirk et al. (1987). STH observations were taken in dry areas free of middle and high clouds along the northwest flank of a TP using the most equatorward SMMR block available; this region lies within the climatologically expected position of the STH. EDZ observations were taken from a subsidence region, also dry and free of high clouds along and south of 5°S from 120°-90°W. AITCZ observations were taken from any area of the ITCZ between 10°N and 5°S with white convective cloud tops. QITCZ observations were taken from areas along the ITCZ between 10°N and 5°S that were clear of white convective cloud tops and usually covered by low clouds over an entire SMMR block.

There were two deficiencies with the data distribution. No observations of QITCZs are taken in May because SMMR data are not available over a QITCZ and because the ITCZ was generally an AITCZ in May. Secondly, Katsaros and Lewis (1986) and Warner (1984) found that SMMR underestimates precipitable water in areas of heavy precipitation. Reduced values of precipitable water were avoided by moving to an adjacent SMMR value that was not influenced by precipitation and using that location for sampling the other data.

For the analysis of SMMR rainrates algorithms used by Katsaros and Lewis (1986) and Warner (1984) were used. The occurrences of rain were stratified by
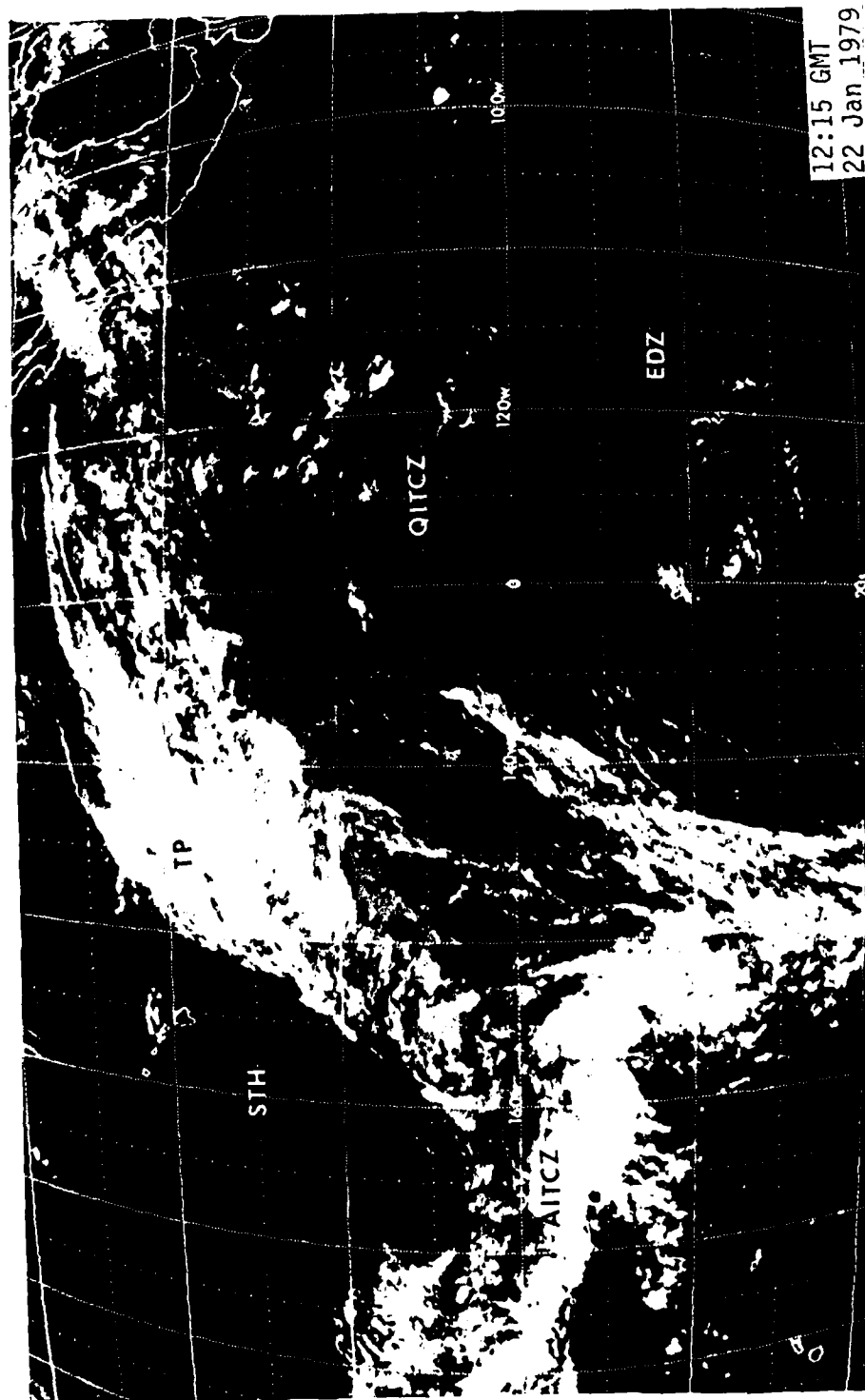
Figure 2. GOES West IR image for 1215 GMT January 22, 1979. Features marked TP, EDZ, STH, AITCZ and QITCZ are described in the text.

month and feature to investigate differences in the highest rainrates and distribution of rainrates. The algorithms use the brightness temperature of the SMMR 37 GHz horizontal channel (T37h). The algorithm shown in equation 1

$$RR = \frac{(T37h) - 190}{10} \tag{1}$$

was used by Katsaros and Lewis (1986) in a study of rainfall off the coast of Washington. This equation specifies the rainrate (RR) in mm hr^{-1} if T37h is given in K. The algorithm shown in equation 2

$$RR = 8.3X10^{-7} \exp^{0.065(T37h)} - 0.1 \tag{2}$$

was used by Warner (1984) in a study of monsoon rainfall off the coast of India, using the same units as equation 1. The two algorithms have different characteristics in rainfall estimation.

The algorithm used by Katsaros and Lewis (1986) was designed to retrieve rainfall from systems that have predominantly steady light rainrates. The highest rainrate values from the algorithm are about 6 mm hr^{-1}. The algorithm used by Warner (1984) was designed for use in systems with heavy rainrates, as in tropical convection. The highest rainrate values from the algorithm are about 18 mm hr^{-1}. The rainrates derived from SMMR are difficult to correlate directly to surface rainrates because they are area averages. The rainrate averaged over the 60 km pixel often results from a small intense rain cell in only one part of the pixel being averaged to a light rainrate for the entire pixel, since the intense rain rarely fills the entire beam; this effect is referred to as the beam filling problem.

The rainrate information will be used only for relative comparisons of the highest rainrate intensities and spatial coverage of the rain between raining features. Rain events were classified as either TP or AITCZ, since these are the only raining features within the study region. TP rain events were classified as such if they were north of 10°N, while ITCZ events occurred south of 10°N, by definition.

CHAPTER V

WATER VAPOR

Atmospheric precipitable water estimates from the several available sources are examined and intercompared over the tropical Pacific Ocean. SMMR precipitable water are compared to TOVS 11, TOVS 12, OLR, and the ECMWF analysis in five different tropical synoptic features during two different months. Quantitative comparisons are made by examination of correlations, mean values and multiple regression. SMMR precipitable water estimates at a resolution of 60 km were demonstrated by Prabhakara et al. (1982) to have a rms deviation from radiosondes of only 2.5 kg m^{-2}. Therefore SMMR precipitable water estimates will be considered "ground truth" and compared to other estimators of precipitable water.

V.1 Correlations Between the Data

A set of 540 collocated observations were collected over the entire period when data are available from SMMR, TOVS 11, TOVS 12, OLR, and the ECMWF analysis. Shown in Table 1 are the results of the cross correlations. The correlations are all greater than 0.4 indicating useful information exists in all of the correlations and they are statistically significant at a level of significance p=0.001. The Student's t tests are used for determining statistical significance in the study and the level of significance represents the probability of observing a sample outcome in random data.

Table 1.   Correlation of SMMR and other precipitable water estimates.

	TOVS 11	TOVS 12	OLR	ECMWF
SMMR	−.61	−.48	−.56	.70
TOVS 11	*	.89	.66	−.56
TOVS 12	*	*	.55	−.44
OLR	*	*	*	−.44

The meteorologically significant contents of the correlations are that each of the channels provides some information about the moisture in the atmosphere when compared to SMMR. Negative correlations indicate the value decreases as precipitable water increases. Correlations of the ECMWF analysis with TOVS and OLR data are slightly worse than the correlations of SMMR with TOVS and OLR data, but not with any statistical confidence. The least representative observations are from OLR data that are not specifically sensitive to precipitable water, and TOVS 12 data that are overly sensitive (contaminated) by minute traces of upper tropospheric moisture. The high TOVS 11 and TOVS 12 correlation was expected, but the high TOVS 11 and TOVS 12 correlation does not carry over to the correlations between SMMR and the two TOVS channels due to the contamination problem.

Scatter plots of the observations are made to study outliers and patterns in the data. Outliers are present in all of the data plots. Some of the outliers are the result of problems with time, space and resolution that are present throughout the data set. The data are sampled in groups of nine observations corresponding to a SMMR block. Accuracy checks were made to ensure no entire blocks of nine observations are outliers. Differences in the times between Nimbus-7, TIROS-N and ECMWF data

can be up to five hours and can also influence spatial problems. Spatial problems result when one type of data is within a feature and other data samples are outside of the feature. Resolution problems result from the 60 km resolution of SMMR and the gridded resolution of the other data sets being at least 250 km. The time, space and resolution problems result in a larger scatter than would be expected if all the data were actually collected in time, space and sensing the same spatial scale.

Figure 3 shows the correlation between TOVS 11 and TOVS 12, which is 0.89. The correlation is high because of the large overlap of the weighting function for the two channels. This correlation is nearly identical to the correlation between the two channels found by Anderson (1986) over the entire tropical Pacific Ocean. Examination of the full range of observations on Fig. 3 shows that synoptic features occupy certain regimes. The wet TP, AITCZ and QITCZ (1, 4 and 5) dominate the colder brightness temperatures in the lower left portion and the dry EDZ and STH dominate the warmer brightness temperatures in the upper right portion of the figure. On the other hand TP observations span the entire range of TOVS 12 and nearly that of TOVS 11. An isolated few EDZ observations are the coldest (wettest) TOVS 12 observations they; are also among the coldest TOVS 11 observations. These observations probably are dominated by a relatively thick upper tropospheric streak of moisture.

The SMMR and TOVS 11 correlation, shown in Fig. 4, is -0.61. As the SMMR estimate of precipitable water increases, TOVS 11 brightness temperature decreases. Although the correlation is good, there is a large scatter, and a given value of SMMR

Figure 3. Plot of TOVS 11 vs. TOVS 12. The numbers represent observations within individual synoptic features: 1=TP, 2=EDZ, 3=STH, 4=AITCZ, 5=QITCZ.
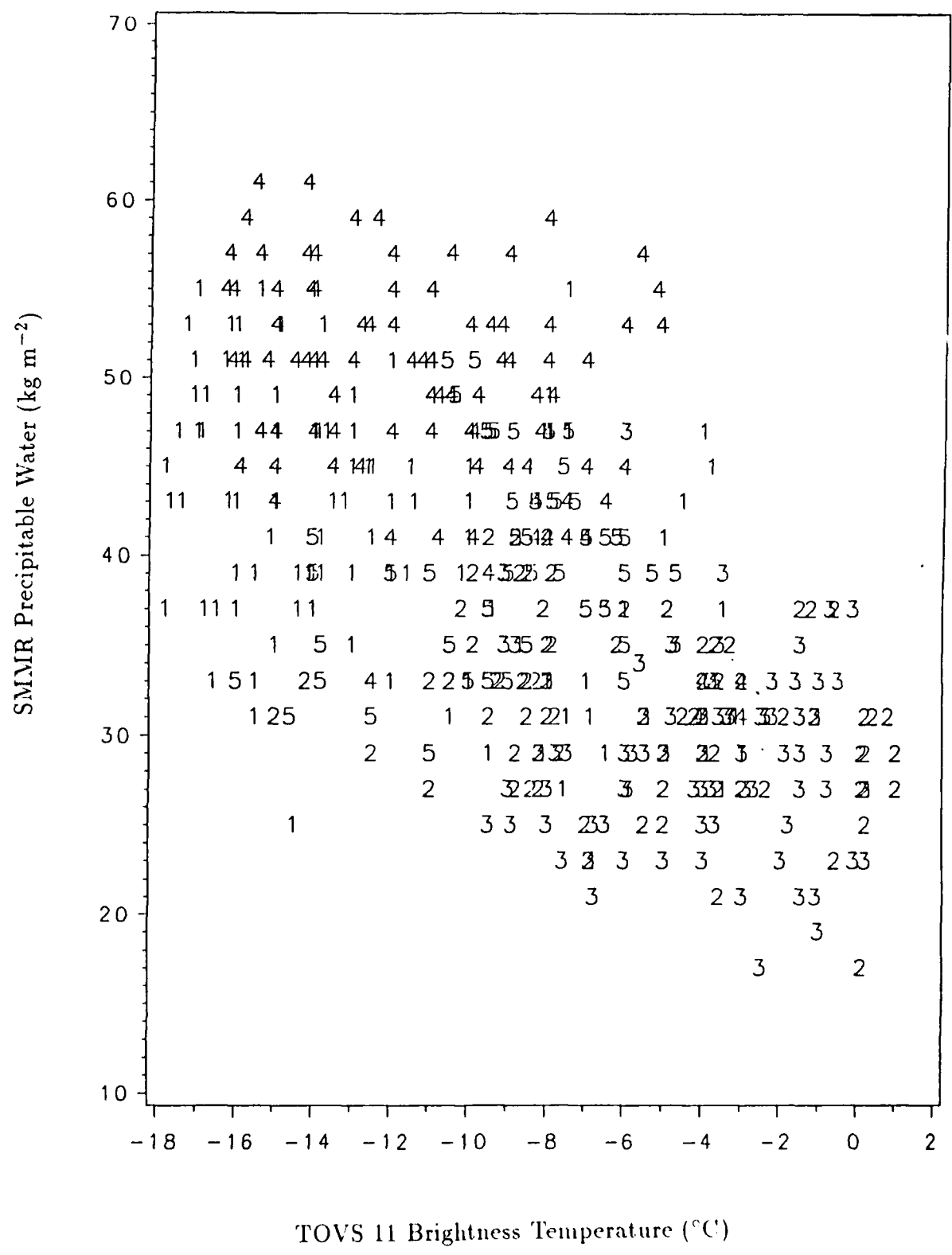
Figure 4. Plot of SMMR vs. TOVS 11. The numbers represent observations within individual synoptic features: 1=TP, 2=EDZ, 3=STH, 4=AITCZ, 5=QITCZ.

can be associated with TOVS 11 observations spanning the entire range of values. The correlations are not better in moist cloudy regions (TPs and AITCZ; 1 and 4) probably because of TOVS sensor limitations. Anderson (1986) describes the process of interpolating TOVS observations from adjacent clear column radiances to complete the data grid. The interpolated values should underestimate systematically the actual precipitable water since they do not sample the highest precipitable water areas, that are the convectively active regions.

The largest moist outliers from the SMMR vs. TOVS 11 plot are in the AITCZ and TP; the largest dry outliers are also in the TP and QITCZ. The AITCZ data on the top right of the plot are from an area that was not characterized by intense ITCZ convection since there were gaps in the clouds on the satellite imagery. Areas with gaps in the ITCZ convection are areas where TOVS 11 data does not provide accurate results. The TP dry outliers at 25 kg m^{-2} of SMMR and $-14.5°C$ of TOVS 11 and wet outliers at 44 kg m^{-2} of SMMR and $-4.5°C$ of TOVS 11 are from areas where the data times do not match well and the TP has moved significantly.

Figure 5 shows the correlation between SMMR and TOVS 12, which is of -0.48. The correlation is weaker than the SMMR and TOVS 11 correlation and any value of SMMR can be associated with TOVS 12 observations spanning almost the entire range of values. SMMR and TOVS 11 correlation is higher because the TOVS 12 channel is more sensitive to insignificant amounts of upper tropospheric moisture. The sensitivity can lead to serious errors in relatively dry atmospheres. Differences in the correlations result primarily from the TOVS 12 channel being unrepresentative
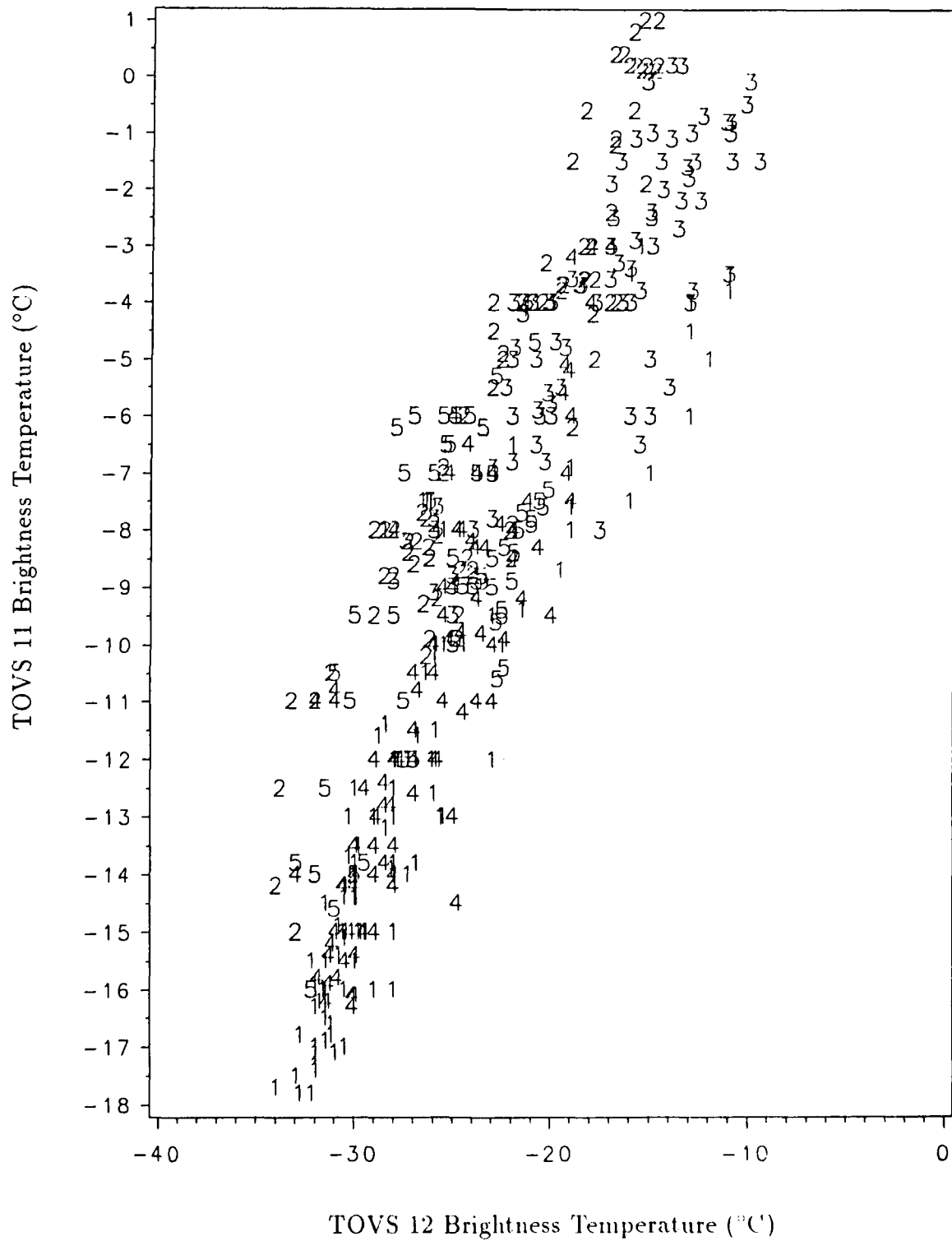
Figure 5. Plot of of SMMR vs. TOVS 12. The numbers represent observations within individual synoptic features: 1=TP, 2=EDZ, 3=STH, 4=AITCZ, 5=QITCZ.

of precipitable water and having a large scatter in areas with a precipitable water contents less than 35 kg m^{-2}. Even though the TOVS 11 and TOVS 12 channels are closely coupled, the correlations with other data are not identical because the TOVS 11 and TOVS 12 differences are systematic.

Outliers of cold TOVS 12 observations on the SMMR vs. TOVS 12 plot are a result of the TOVS 12 sensitivity to upper tropospheric moisture. When SMMR values are low (dry) and TOVS 12 values are cold (wet) the atmosphere is dry and TOVS 12 data are detecting upper tropospheric moisture. When SMMR values are greater than 40 kg m^{-2} and TOVS 12 values are warm (dry) most of the moisture is in the layers below where TOVS 12 data are sensitive to moisture. The observations from areas of the AITCZ where TOVS 12 temperatures are about $-20°C$ occurred in AITCZs where significant breaks in the cloud cover existed. These areas represent regions where TOVS 12 does not provide accurate results. Many of these data points occur in the same location where TOVS 11 does not provide accurate results.

Figure 6 shows the correlation between SMMR and OLR, which is -0.56. The correlation indicates as precipitable water increases OLR decreases (high cloud cover increases). Observations in the STH and EDZ have low SMMR precipitable water content and high OLR values. These areas with low precipitable water are clear and the radiating surface is near sea level and warm. Correlation in the low (less than 220 W m^{-2}) OLR (wet) regions of the TP and AITCZ have a large scatter and the highest precipitable water values do not correspond to the lowest OLR values. The SMMR values near 40 kg m^{-2} and OLR values near 180 W m^{-2} occurred very close
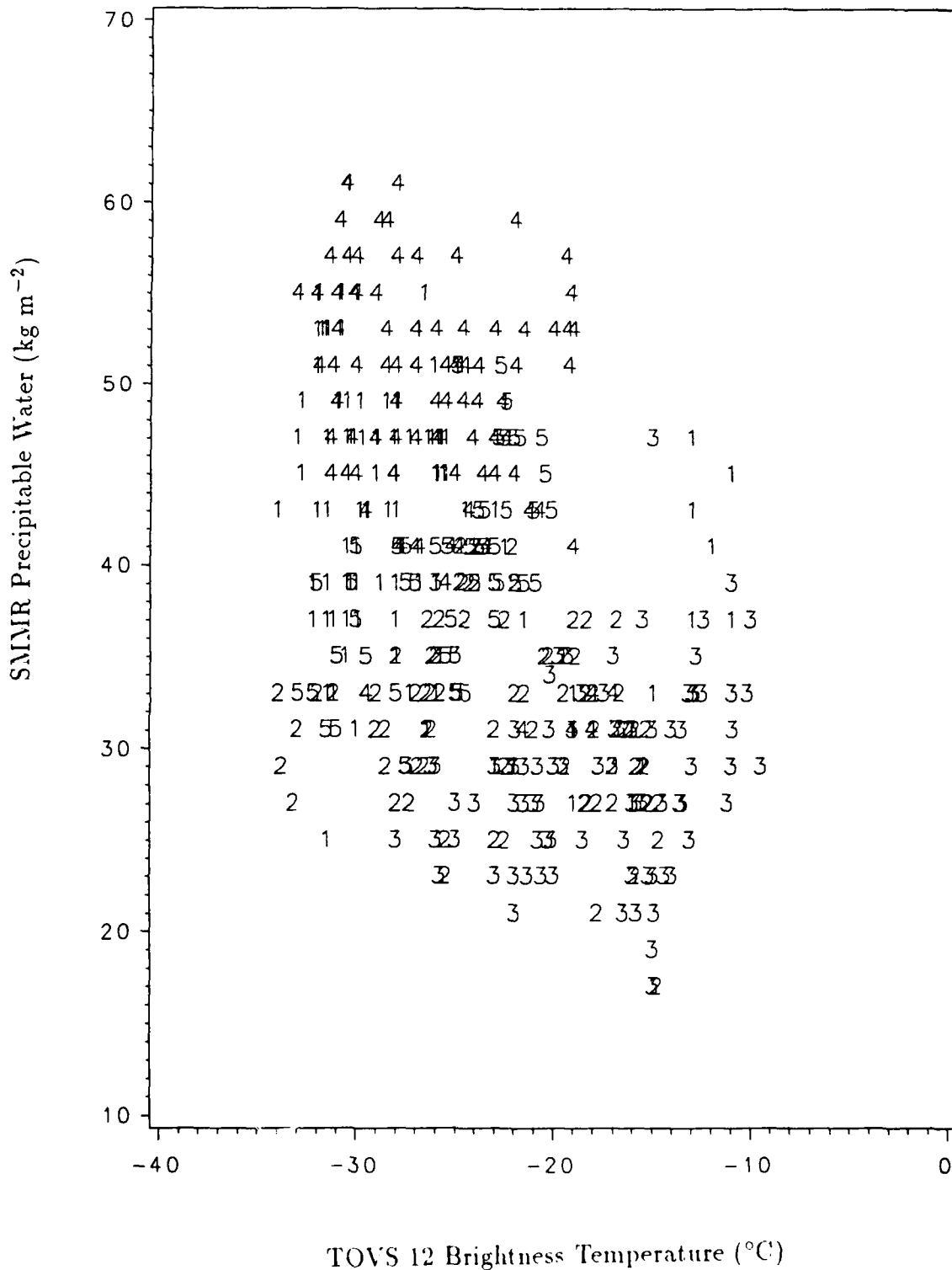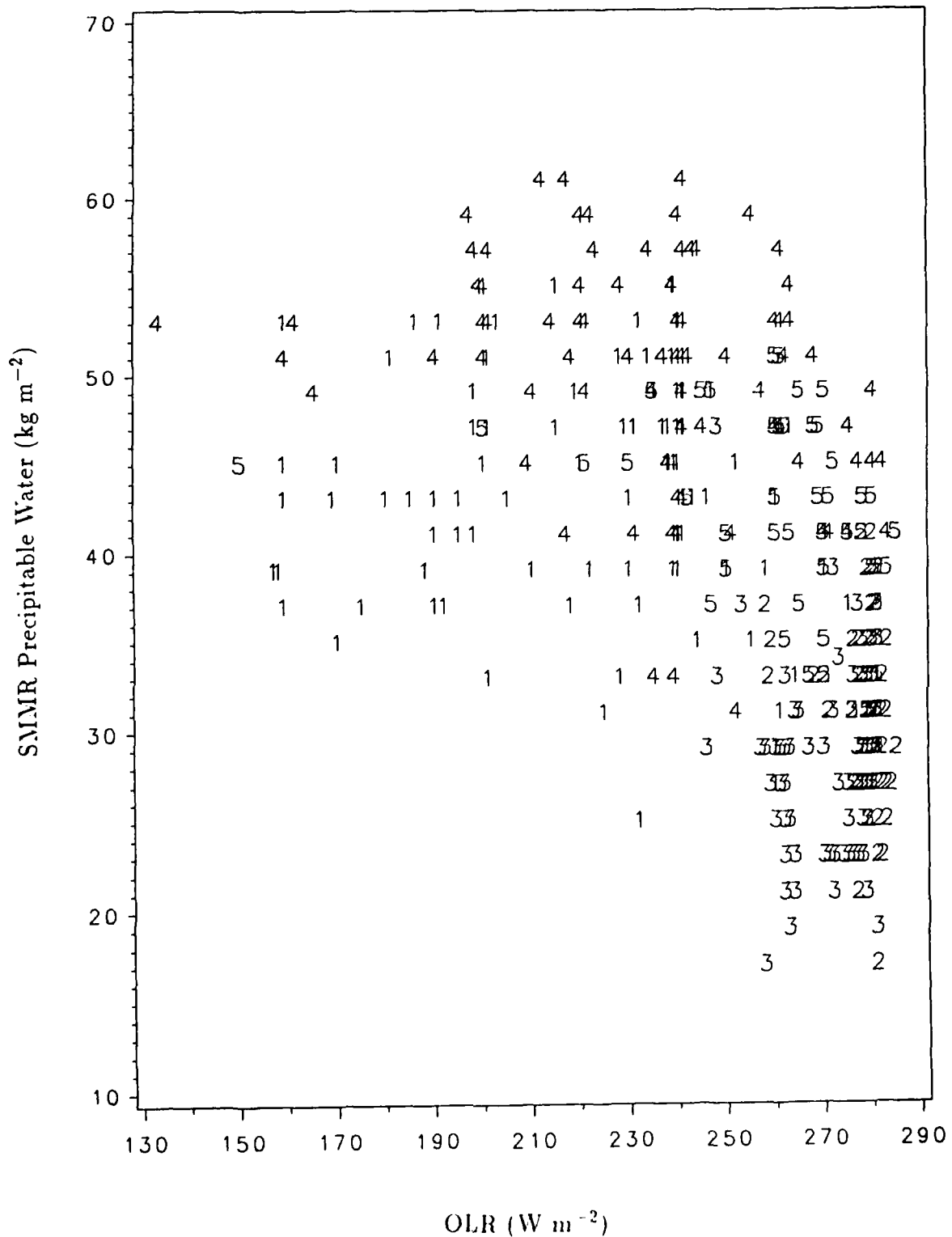
Figure 6.   Plot of SMMR vs. OLR. The numbers represent observations within individual synoptic features: 1=TP, 2=EDZ, 3=STH, 4=AITCZ, 5=QITCZ.

to areas of heavy precipitation, mostly in TPs, so the SMMR values are contaminated and unrepresentative of the actual precipitable water values. The highest (dry) values of OLR, mostly from the EDZ and STH, span a 40 kg m^{-2} range. Although the range of SMMR data are large the OLR varies only about 20 W m^{-2}. The small OLR variations are due to the clear skies in the STH and EDZ and the resulting OLR coming from the tops of low trade wind clouds or the ocean surface that have high stable OLR values. In these regions of normal subsidence there is little relation between the variations of moisture and the absence of cloud. The lowest (wet) values of OLR, mostly from the TP and AITCZ, occupy a 15 kg m^{-2} range (excluding many SMMR values erroneously low) of SMMR precipitable water estimates. Cadet (1983) used OLR for making moisture estimates for the ECMWF analysis where other data are not available. The current analysis indicates that low OLR values do not guarantee a deep layer of moisture or account for the variability in the amount of moisture. If more advanced techniques are available the current results would discourage use of OLR as input for moisture to the ECMWF analysis.

The SMMR and ECMWF correlation shown in Fig. 7 is the best correlation of any data with SMMR (0.70), even though some ECMWF values span most of the range of SMMR. The correlation indicates that as precipitable water increases so does the ECMWF analysis of precipitable water; but the ECMWF has a dry bias of about 0.5 cm of precipitable water, particularly in wet atmospheres. Data from the AITCZ have the highest precipitable water contents, while data from the EDZ and STH have the lowest precipitable water contents.
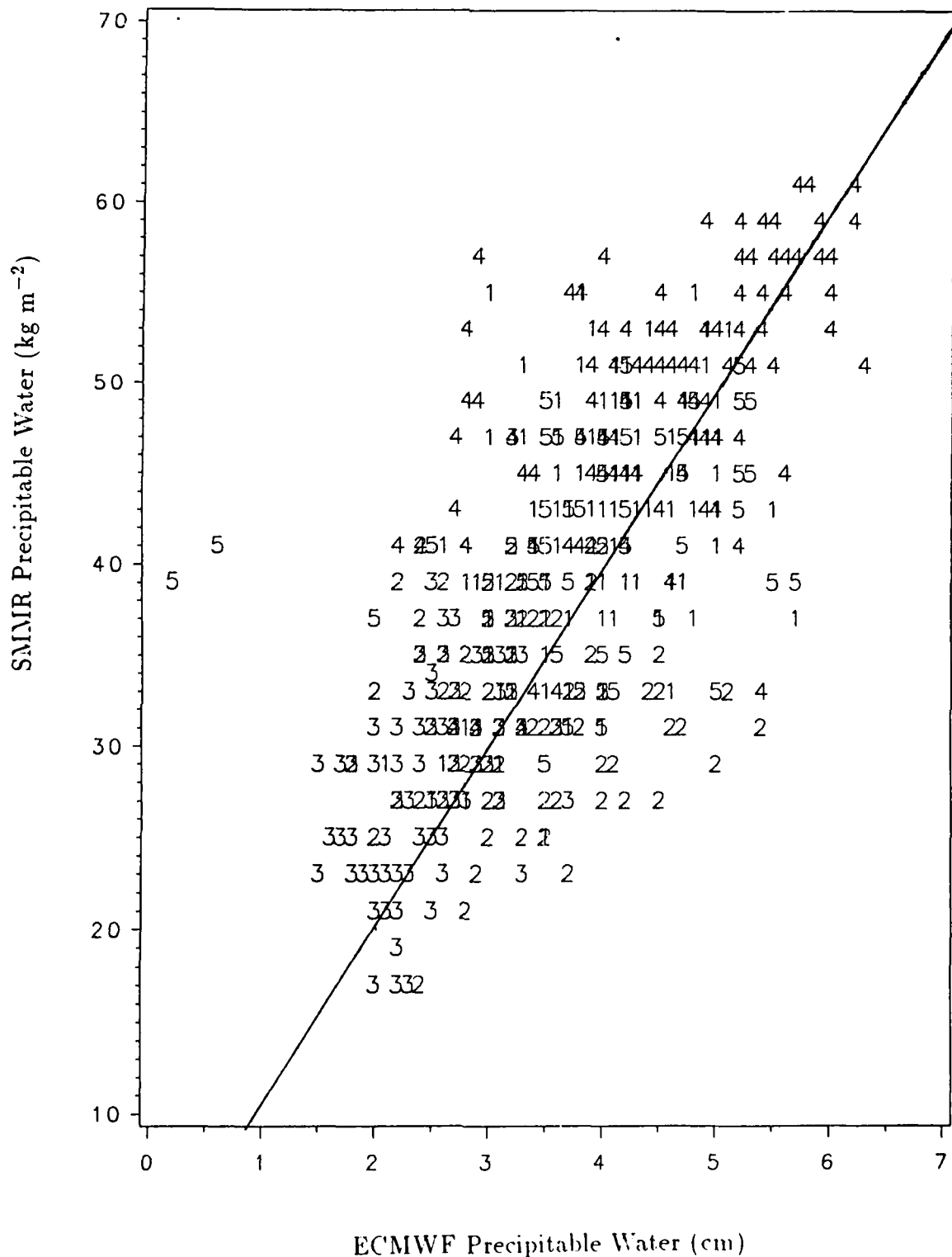
Figure 7. Plot of SMMR vs. ECMWF. The straight line would be a perfect fit and 10 kg m^{-2} of precipitable water is equivalent to 1 cm of precipitable water. The numbers represent observations within individual synoptic features: 1=TP, 2=EDZ, 3=STH, 4=AITCZ, 5=QITCZ.

The two outliers on the far left of Fig. 7 occurred in a QITCZ and demonstrate one of the problems of the ECMWF analysis. The ECMWF analysis frequently reduces the moisture on and near the ITCZ to values that are unreasonable. The reduction in moisture usually occurs in clear areas and demonstrates where the ECMWF analysis could benefit from input of satellite moisture data that are usually reliable in clear areas. The AITCZ outliers at 53 kg m^{-2} of SMMR and 3.0 cm of ECMWF occurred in an AITCZ where the clouds were broken and not the usual solid cloud cover. In these areas TOVS and OLR data are middle range values and not representative of the wet SMMR values. These data points are also extreme examples of the underprediction of precipitable water by the ECMWF in the AITCZ. In the EDZ at $^{\circ}8$ kg m^{-2} of SMMR and 4.8 cm of ECMWF precipitable water, the ECMWF analysis consistently overpredicts the precipitable water in an area where the highest SMMR precipitable water estimates are 40 kg m^{-2}. In the STH the ECMWF analysis consistently underpredicts the precipitable water by 0.5 cm of precipitable water. The TOVS and OLR data in the EDZ and STH are generally well correlated with the SMMR precipitable water values. In the TP the ECMWF data are reasonable with the outliers probably the result of differences in resolution.

Lines are drawn around the values within each feature to depict the representative distribution for each feature. The lines in Fig. 8 encircle the representative precipitable water values of each synoptic feature, which are plotted in Fig. 7. The shape of the line provides an estimate of the precipitable water values present in each feature. Circles are areas where predictions are difficult since the estimation errors

ECMWF Precipitable Water (cm)
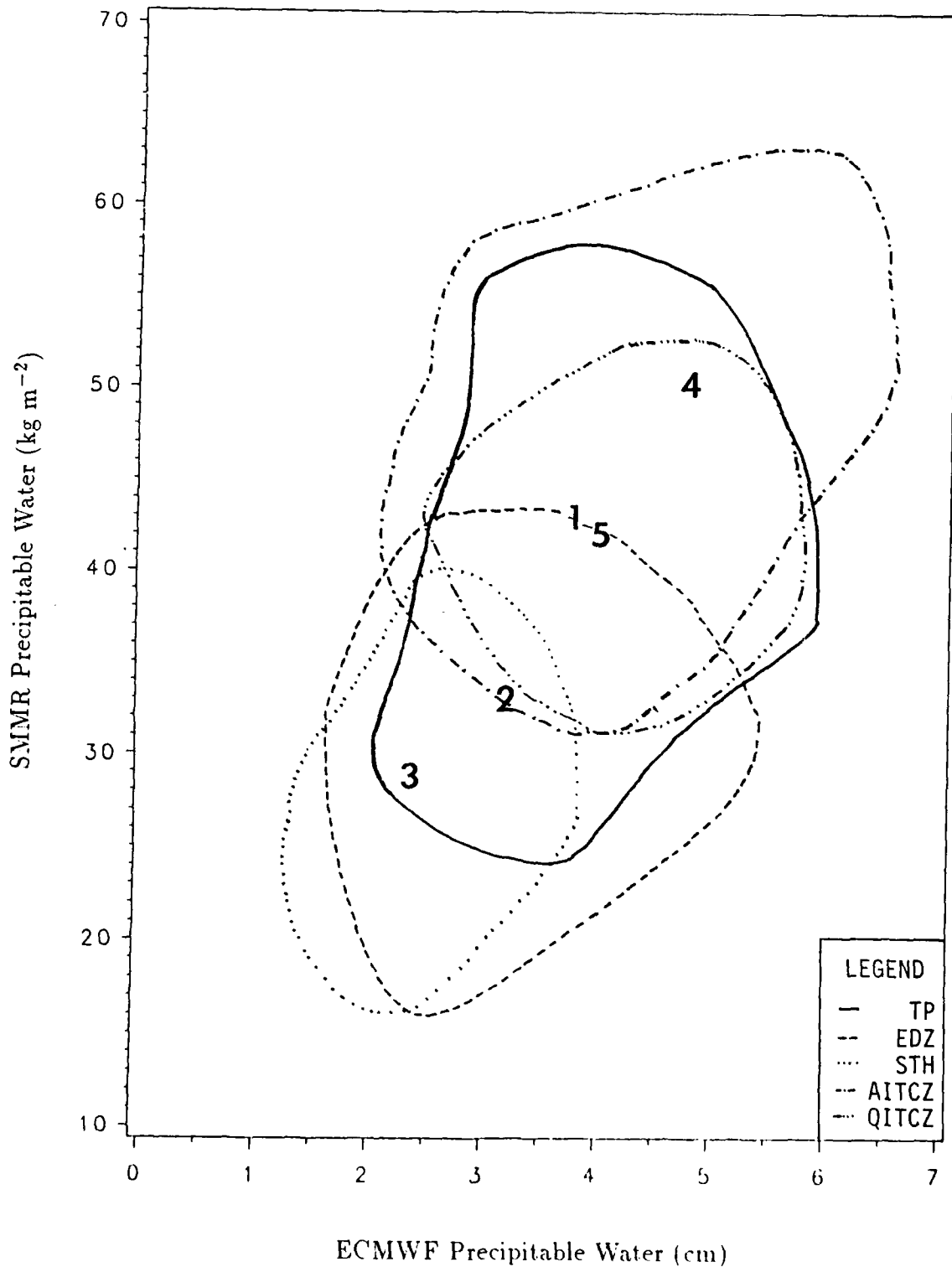
Figure 8. Schematic replot of SMMR vs. ECMWF, from Fig. 7, with numbers
deleted. The deleted numbers are replaced by lines that encircle the
precipitable water values within each feature. The numbers identify the
mean values of SMMR and ECMWF within individual synoptic features:
1=TP, 2=EDZ, 3=STH, 4=AITCZ and 5=QITCZ.

are as great as the range of data. The ellipses are areas where predictions are better
since the range of the data is greater than the estimation errors.

There are two main problems with all the correlations. First, all of the plots
of SMMR vs. the other data display a large scatter, where observations associated
with a specific SMMR value will span almost the entire range of that observations
data set. Second the TOVS 11, TOVS 12 and OLR data are not indicators of
only total precipitable water because the instruments are sensitive to other effects
in the atmosphere, such as clouds or the vertical distribution of locally high relative
humidity.

The correlation between OLR and TOVS 11 of 0.66 in Fig. 9 shows that as the
TOVS 11 brightness temperature decreases, indicating more moisture, OLR decreases,
indicating increased cloudiness. The correlation between OLR and TOVS 12 of 0.55
shown in Fig. 10 is similar to the OLR and TOVS 11 correlation. The TOVS 12
correlation is lower due to the greater variability in the signal as a result of the
sensitivity to upper tropospheric moisture. Both of these correlations have a problem
with scatter where a given TOVS brightness temperatures are present in the entire
range of OLR data. OLR observations generally provide threshold information; the
smaller OLR (that is more and higher convective clouds) the less likely that other
estimators will indicate extremely dry atmospheric columns.

Outliers from the AITCZ in the lower right of both the OLR vs. TOVS plots
occurred in areas adjacent to the AITCZ or in an AITCZ that had large gaps in
convective cloud tops. The large variation in TOVS values from the EDZ and STH

Figure 9. Plot of OLR vs. TOVS 11. The numbers represent observations within individual synoptic features: 1=TP, 2=EDZ, 3=STH, 4=AITCZ, 5=QITCZ.
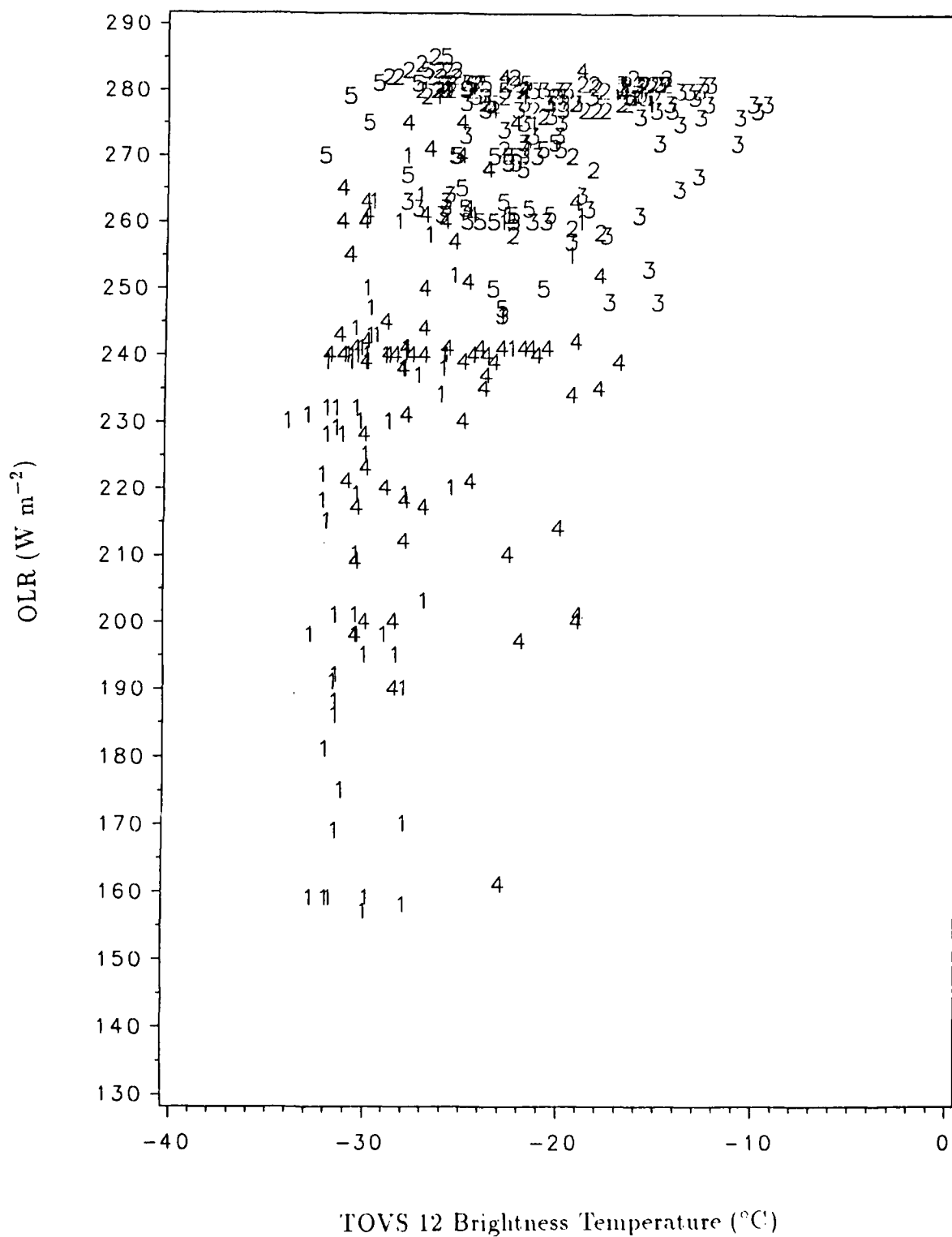
Figure 10. Plot of OLR vs. TOVS 12. The numbers represent observations within individual synoptic features: 1=TP, 2=EDZ, 3=STH, 4=AITCZ, 5=QITCZ.

occur because the OLR values are consistent in clear areas while the TOVS channels are detecting variations in the level of moisture.

The correlation between TOVS 11 and ECMWF of −0.56 in Fig. 11 shows that as ECMWF precipitable water increases TOVS 11 brightness temperature decreases, indicating increased moisture. The two observations on the far left of the figure are from a QITCZ where the SMMR precipitable water content was about 40 kg m^{-2} and represent a problem with the ECMWF analysis.

The correlation of TOVS 12 and ECMWF is −0.44 as shown in Fig. 12. The OLR and ECMWF correlation is −0.44 as shown in Fig. 13. Both of these are low correlations and have a large scatter, so the most useful information is in the sign. The sign indicates as the ECMWF precipitable water increases the TOVS 12 brightness temperature and the amount of OLR both decrease, indicating increased moisture. All of these plots have the problem with scatter that result from deficiencies in the ECMWF analysis.

Separating the data by feature was done to investigate the correlations within each feature. Table 2 shows the correlations within features. A $p=0.05$ was used to estimate statistical significance. Half of the data correlations within the features were not significantly different from zero. This is due only in part to small sample size as the data set was stratified. Correlations not statistically different from zero are indicated by an "N" in Table 2. Correlations between the data for all features, although significantly different from zero, are meteorologically significant in only a few cases.

Figure 11. Plot of TOVS 11 vs. ECMWF. The numbers represent observations within individual synoptic features: 1=TP, 2=EDZ, 3=STH, 4=AITCZ, 5=QITCZ.

Figure 12.   Plot of TOVS 12 vs. ECMWF. The numbers represent observations within individual synoptic features: 1=TP, 2=EDZ, 3=STH, 4=AITCZ, 5=QITCZ.
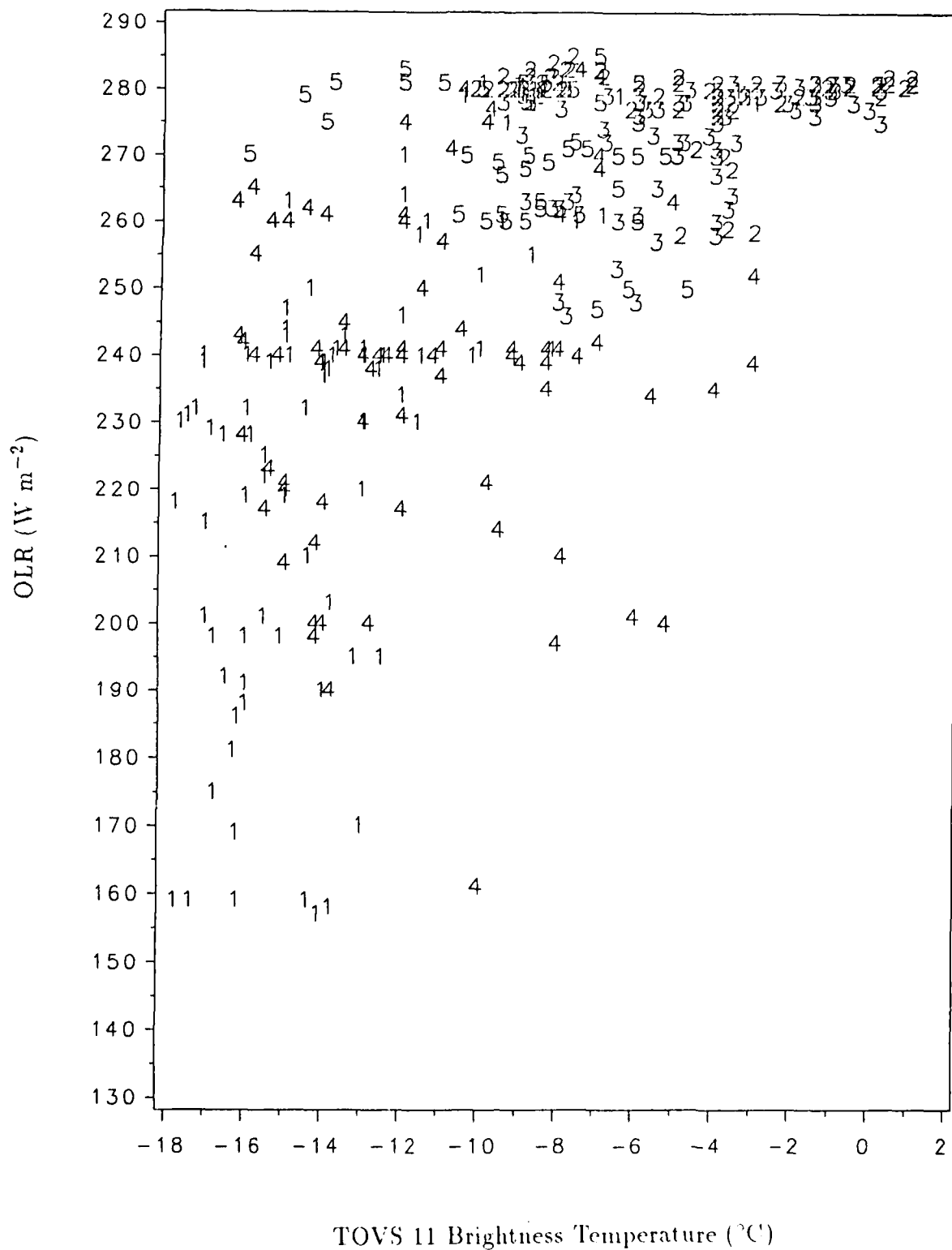
Figure 13. Plot of OLR vs. ECMWF. The numbers represent observations within individual synoptic features: 1=TP, 2=EDZ, 3=STH, 4=AITCZ, 5=QITCZ.

Table 2. Correlation of SMMR to other precipitable water estimates stratified by synoptic feature. Correlations not statistically different from zero are indicated by an "N".

TP

	TOVS 11	TOVS 12	OLR	ECMWF
SMMR	−.35	−.36	−.28	.46
TOVS 11	*	.90	.60	N
TOVS 12	*	*	.55	N
OLR	*	*	*	N

EDZ

	TOVS 11	TOVS 12	OLR	ECMWF
SMMR	−.33	N	N	N
TOVS 11	*	.93	N	N
TOVS 12	*	*	N	N
OLR	*	*	*	N

STH

	TOVS 11	TOVS 12	OLR	ECMWF
SMMR	N	N	N	.49
TOVS 11	*	.84	.44	N
TOVS 12	*	*	N	N
OLR	*	*	*	N

AITCZ

	TOVS 11	TOVS 12	OLR	ECMWF
SMMR	−.48	−.39	N	.54
TOVS 11	*	.87	N	−.55
TOVS 12	*	*	N	−.43
OLR	*	*	*	N

QITCZ

	TOVS 11	TOVS 12	OLR	ECMWF
SMMR	N	.61	−.40	N
TOVS 11	*	.67	N	−.39
TOVS 12	*	*	N	N
OLR	*	*	*	−.47

The main feature of the correlations between SMMR and the other data in Table 1 are the interregional variations, while Table 2 represents intra-system variations associated with synoptic structure. The data are most successful at quantifying moisture where a large variation in moisture exists. Large variations in moisture exist between different synoptic features and within TPs and within the AITCZ. The weakest correlations and fewest significant correlations occurred in the EDZ where the variations in the moisture are small.

Variations in the correlations between features are well demonstrated by the correlation between SMMR and TOVS 11. The overall correlation is -0.61, and the best correlation within a feature between SMMR and TOVS 11 is -0.48, within the AITCZ. Three of the five correlations between SMMR and TOVS 11 and within features are significantly different from zero, but they explain only modest fractions of the within feature variations. Another example of variability in the overall correlation is the correlation of SMMR and the ECMWF analysis. The overall correlation is 0.70, but when separated by feature only three out of five feature correlations are significantly different from zero. One conclusion that can be drawn is the data can distinguish the large variations between synoptic features, but once within a synoptic feature the data have difficulty in distinguishing small, but meteorologically important variations in moisture.

Stratified by synoptic feature the correlations between SMMR and TOVS 12 are generally in line with the overall correlation, but there is an exception in a QITCZ. The overall correlation between SMMR and TOVS 12 is -0.48. In the

QITCZ (Fig. 14) the correlation is a statistically significant 0.61; a larger correlation, with a surprising change in sign. The change in sign is due most likely to the moisture TOVS 12 data are detecting. TOVS 12 has its peak weighting function at 500 mb, but is sensitive to insignificant amounts of upper tropospheric moisture, while SMMR responds more directly to integrated precipitable water. Therefore in some of the observations SMMR was estimating large amounts of precipitable water, but most of this moisture appeared at low levels and not detected by TOVS 12. The result is a moist SMMR precipitable water amount of about 50 kg m^{-2} and a warm, relatively dry, TOVS 12 brightness temperature of about -24 °C. In other instances the SMMR was indicating a relatively dry 35 kg m^{-2} of precipitable water and TOVS 12 was indicating a cool, relatively wet, brightness temperature of about -30 °C. The instances where TOVS 12 indicates high atmospheric moisture content in a relatively dry atmosphere were found by Blackwell (1987) to be from small amounts of precipitable water at very cold temperatures in the upper troposphere that the TOVS 12 channel detects. In this case the moisture could of been put into the upper troposphere by small scale convection that did not increase the moisture content of the entire atmosphere and therefore did not increase the SMMR precipitable water amount.

The overall correlation between TOVS 11 and TOVS 12 varies depending on feature. The correlation varies between different features depending on the upper level moisture TOVS 12 detects. The highest correlation is 0.93 for the EDZ, a very stable synoptic feature, and the lowest correlation is 0.87 for the QITCZ. Variability
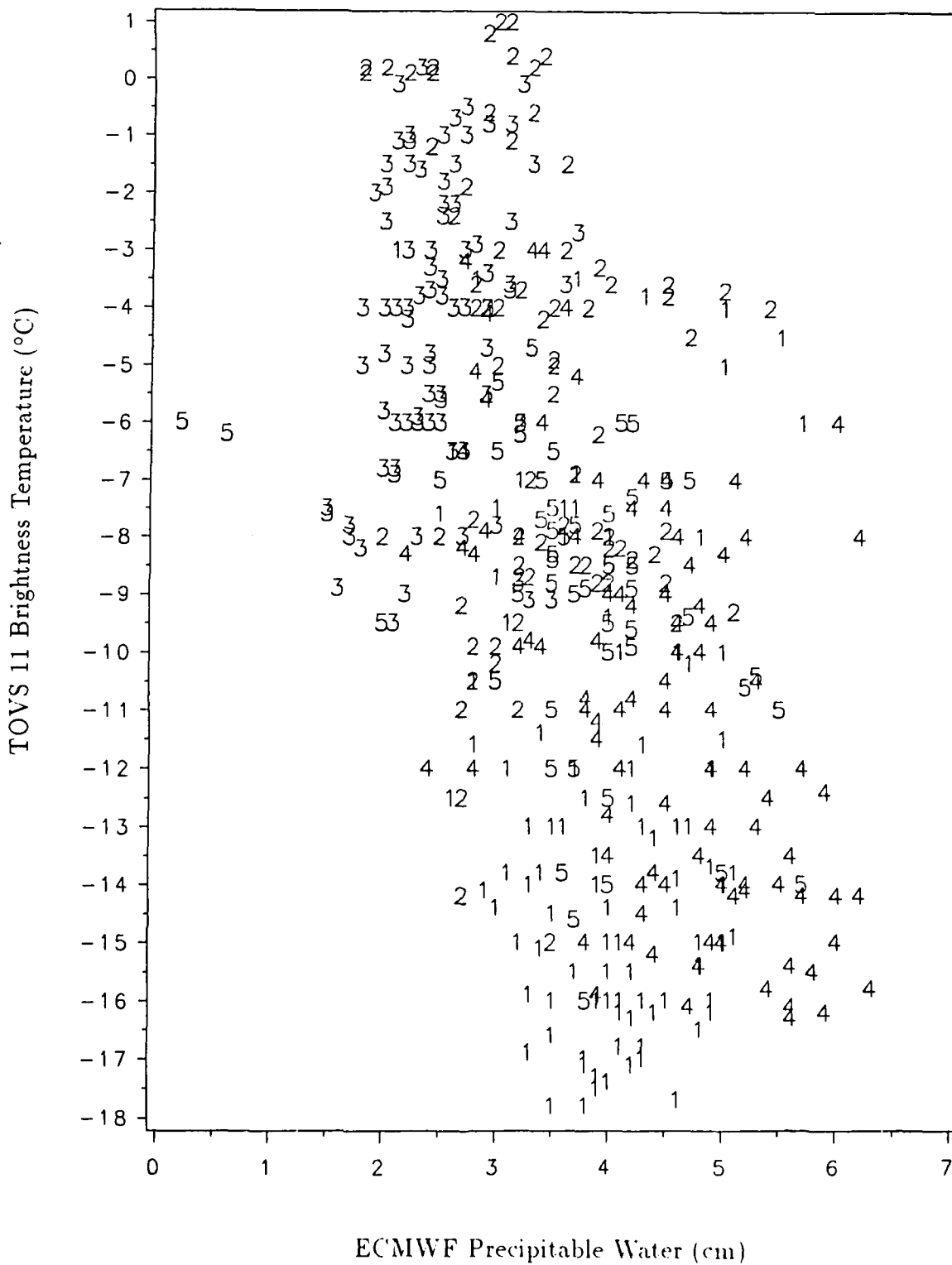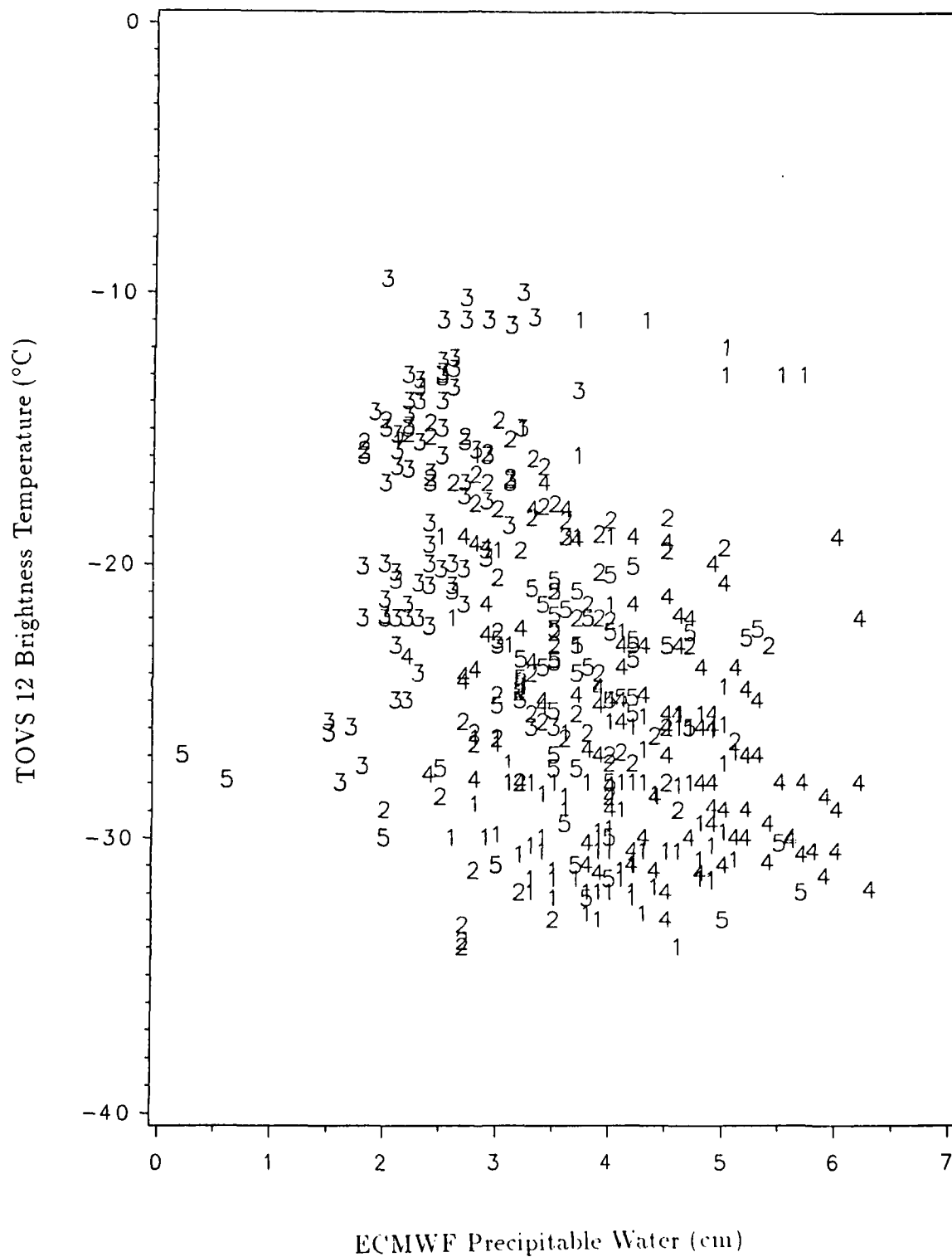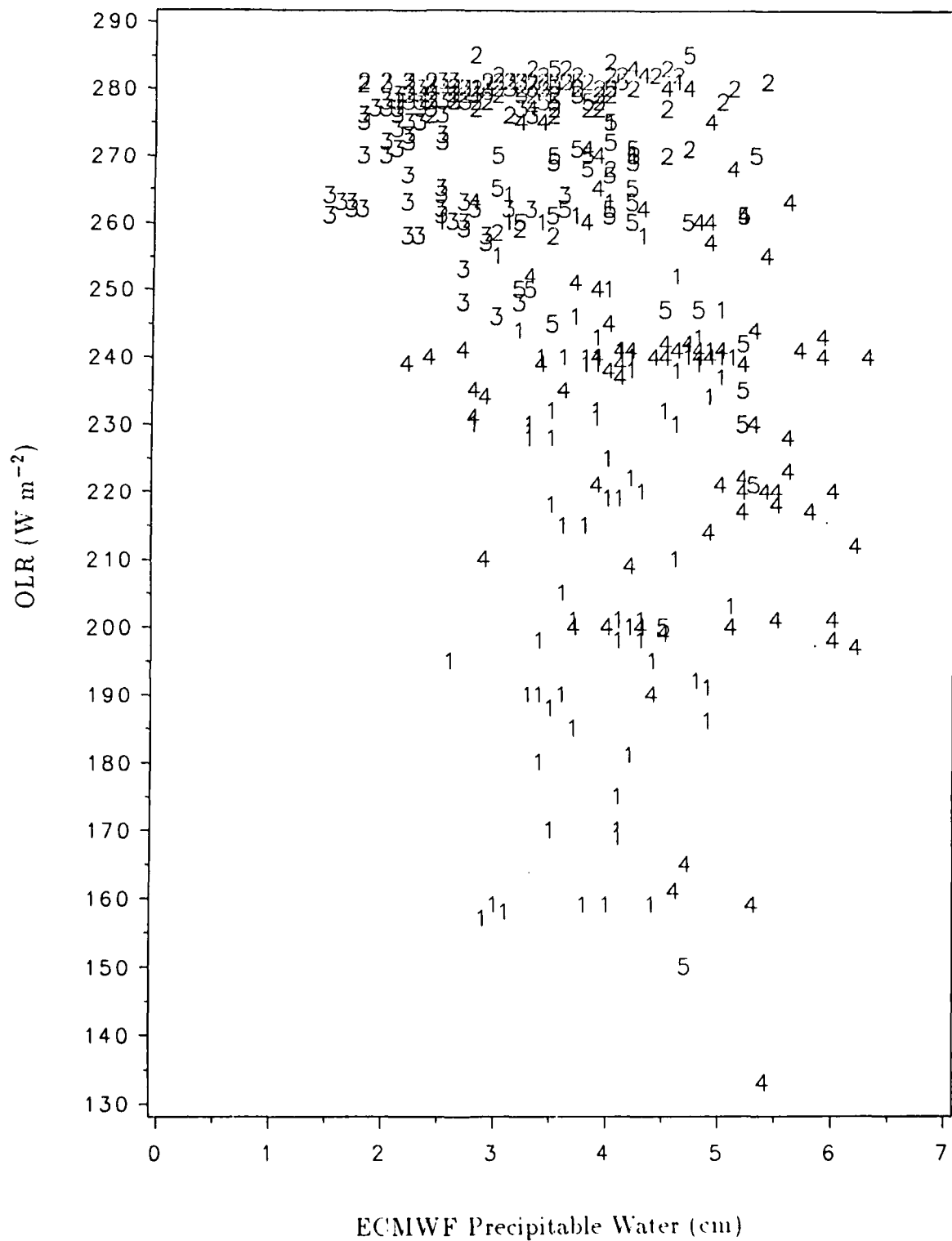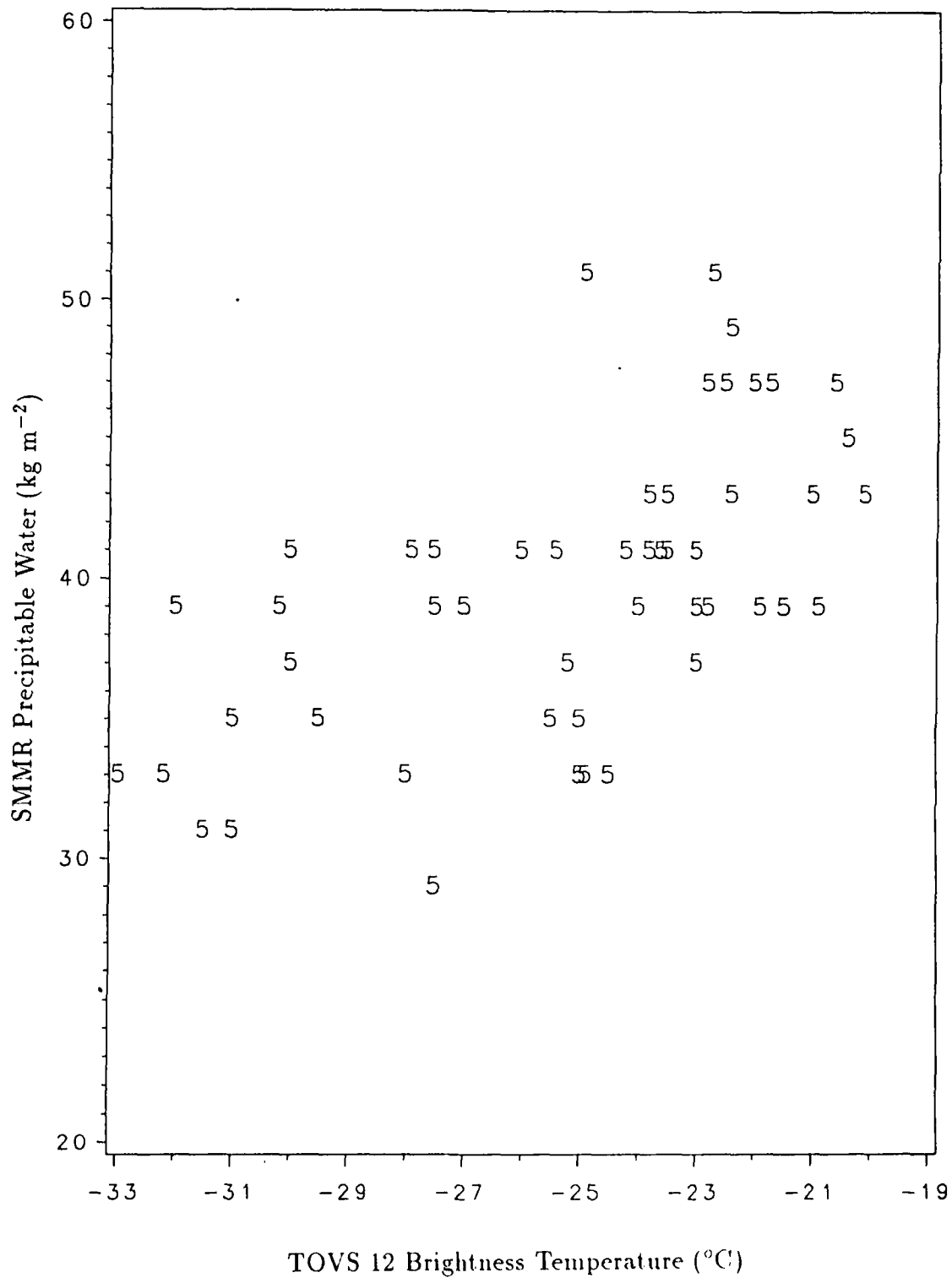
Figure 14. Plot of SMMR vs. TOVS 12 in a QITCZ. The numbers represent observations within individual synoptic features: 1=TP, 2=EDZ, 3=STH, 4=AITCZ, 5=QITCZ.

Table 3.   Correlation of SMMR to other precipitable water estimates stratified by
month.

January

	TOVS 11	TOVS 12	OLR	ECMWF
SMMR	−.59	−.42	−.51	.66
TOVS 11	*	.86	.60	−.52
TOVS 12	*	*	.46	−.35
OLR	*	*	*	−.40

May

	TOVS 11	TOVS 12	OLR	ECMWF
SMMR	−.65	−.62	−.64	.81
TOVS 11	*	.96	.78	−.63
TOVS 12	*	*	.73	−.61
OLR	*	*	*	−.54

in the amount of upper tropospheric moisture in a QITCZ is probably what lowers

the TOVS 11 and TOVS 12 correlation.

The data are stratified by month for the analysis in Table 3 to determine

if there are significant differences between January and May. Stratified by month

the overall correlation between TOVS 11 and TOVS 12 increases to 0.96 in May and

decreases to 0.86 in January. The reduction in correlation in January could result from

increased synoptic scale activity present in January. All other data when separated

into January and May showed higher correlations in May. The higher correlations

in May might indicate the lower synoptic variability of the period. During the May

period the transient synoptic systems were infrequent and the other features appeared

more stable providing a consistent moisture content.

V.2 Synoptic Structure of the Data

The mean values for SMMR, TOVS 11, TOVS 12, OLR, and the ECMWF analysis were stratified to see if differences in day, night, months and features were statistically detectable. A level of significance $p=0.05$ was used to determine meaningful statistical differences. Day and night differences in moisture were not considered statistically different in SMMR, TOVS 11 and the ECMWF analysis. The OLR day and night differences which were found are known to exist in OLR due to diurnal variations in typical cloud cover.

Differences in the mean values of precipitable water between features for the months of January and May are not significantly different in SMMR, TOVS 11, TOVS 12 or the ECMWF analysis. This could be due to the steadiness of the tropical environment and the method of sampling which used cloud features to identify areas to sample.

Table 4 stratifies mean values of precipitable water and standard deviations with respect to the five features. Overall, the mean values of the TP and AITCZ are higher and the standard deviations are larger. The EDZ, STH and QITCZ have lower mean values and smaller standard deviations. The lower standard deviations are due to the steady moisture content of the EDZ, STH and QITCZ, while the active TP and AITCZ have large variations in moisture content.

The mean values and standard deviations of SMMR and the ECMWF analysis follow a similar pattern within features. The mean values of these two estimates in the TP and QITCZ are not statistically different, using a $p=0.05$, implying that these

Table 4. Mean values and standard deviations of precipitable water stratified by synoptic feature. Units are SMMR (kg m^{-2}), TOVS (°C), OLR (W m^{-2}) and ECMWF (cm).

TP

	Mean	Standard Deviation
SMMR	42.1	6.9
TOVS 11	−12.6	3.9
TOVS 12	−27.0	5.6
OLR	222.0	33.0
ECMWF	3.9	0.7

EDZ

	Mean	Standard Deviation
SMMR	31.9	4.9
TOVS 11	−5.6	3.9
TOVS 12	−22.4	5.2
OLR	279.0	5.0
ECMWF	3.3	0.8

STH

	Mean	Standard Deviation
SMMR	28.1	5.3
TOVS 11	−4.2	2.5
TOVS 12	−18.0	4.7
OLR	272.0	9.0
ECMWF	2.5	0.5

AITCZ

	Mean	Standard Deviation
SMMR	49.4	7.0
TOVS 11	−11.0	3.3
TOVS 12	−26.2	3.9
OLR	235.0	29.0
ECMWF	4.5	1.0

QITCZ

	Mean	Standard Deviation
SMMR	41.0	5.4
TOVS 11	−9.1	2.6
TOVS 12	−25.1	3.5
OLR	263.0	23.0
ECMWF	3.8	1.0

two features have a similar moisture content. The only difference was the TP had a larger standard deviation than a QITCZ. The larger standard deviation of the TPs results from the large variations in moisture under the cloud shield. Some areas of the cloud shield are moist regions of active convection while other regions are cirrus blowoff with no deep moisture layer. TOVS 11 mean values are significantly different from each other in all five features. TOVS 12 mean values in the TP and AITCZ are not statistically different. The lack of statistical difference is due probably to the upper tropospheric moisture that TOVS 12 data are sensing in these active weather systems. The OLR data mean values are statistically different from each other for all five features. Thus only OLR and TOVS 11 data are capable of differentiating all synoptic features.

V.3   Prediction of Precipitable Water

Prediction of precipitable water is accomplished through multiple regression of TOVS 11, TOVS 12, OLR and the ECMWF analysis, using SMMR as a ground truth. The prediction of precipitable water is important because there is a longer and more comprehensive data set available using TOVS, OLR and ECMWF data. The longer data set can be used for studies of precipitable water before SMMR was available and for times when SMMR is less reliable. After analysis of all models a multiple regression equation that used ECMWF, TOVS 11, TOVS 12 and OLR to predict SMMR was selected as the best (highest explained variation, while still being statistically robust). Selection of the best model was accomplished by comparing the coefficients of determination (R^2), the $C(P)$ statistic and parameter estimates.

The C(P) statistic measures the total squared error for a subset model containing P independent variables and identifies the best model when it reaches a minimum. The best single variable model used the ECMWF analysis and had a $R^2=0.55$. The best two variable models are not easily distinguished since a model based on ECMWF and TOVS 11 had an $R^2=0.618$ and one based on ECMWF and OLR had an $R^2=0.626$. The best three variable model used ECMWF, but various combinations of TOVS 11, TOVS 12 and OLR resulted in variations of R^2 between only 0.627 and 0.655. The two and three variable model differences are statistically measurable, but probably represent sample fluctuations and would be meaningless with an independent data set. The four variable model shown as Equation 3: provides the best prediction of SMMR (referred to as PSMMR). The predictors are listed in decreasing order of importance.

$$\text{PSMMR (kg m}^{-2}) = 41.4 + 5.62(\text{ECMWF cm}) - 1.25(\text{TOVS 11 °C})$$
$$+ 0.78(\text{TOVS 12 °C}) - 0.055(\text{OLR W m}^{-2}) \quad (3)$$

Of the inputs to the multiple regression equation the ECMWF analysis has the greatest weight. The model predicted SMMR with a coefficient of determination $R^2=0.67$, the C(P) was the lowest of all models and all parameter estimates were statistically significant (p=0.001). Study of the model reveals the sign of the TOVS 12 parameter is opposite of physical logic. TOVS 12 values range from -30 to -10 °C, and the colder temperatures normally imply increased precipitable water, but an value of -30 °C would result in a decrease in the precipitable water amount. The sign of TOVS 12 in the regression equation implies that cold TOVS 12 decreases PSMMR,

and may reflect the response of the linear regression equation to the high variability of TOVS 12 data. OLR values also decrease the predicted amount of precipitable water, but the lower (wet) OLR values decrease the prediction less, which is physically reasonable.

To use the model insert values for ECMWF precipitable water, TOVS 11, TOVS 12 and OLR using the units indicated in equation 3. The result is a value for precipitable water calculated in units of kg m^{-2}. An example of PSMMR using actual observation from within the STH is shown in Equation 4.

$$PSMMR = 41.4 + 5.62(2.0 \text{ cm}) - 1.25(-11.6 \text{ °C})$$

$$+ 0.78(-28.5 \text{ °C}) - 0.055(278 \text{ W m}^{-2}) \tag{4}$$

The results are in Equation 5:

$$29.63 \text{ kg m}^{-2} = 41.4 + 11.24 + 14.5 - 22.23 - 15.29 \tag{5}$$

In this scale, the contribution of each of the four estimators is of the approximate same size. The SMMR estimate in this example is 24 kg m^{-2} and shows how PSMMR tends to overpredict in dry areas. In the STH case most of the overprediction could be a result of the -28.5°C (cold, and typical of the STH) TOVS 12 temperature; if this temperature were an average TOVS 12 temperature of -22.0°C the PSMMR would be 24.6 kg m^{-2}, a more accurate value.

An example of PSMMR using data from the QITCZ is shown in Equation 6.

$$PSMMR = 41.4 + 5.62(3.4 \text{ cm}) - 1.25(-15.5 \text{ °C})$$

$$+ 0.78(-30.4 \text{ °C}) - 0.055(240 \text{ W m}^{-2}) \tag{6}$$

The results are in Equation 7:

$$43.0 \text{ kg m}^{-2} = 41.4 + 19.1 + 19.4 - 23.7 - 13.2 \tag{7}$$

The SMMR estimate in this example was 55 kg m^{-2} and shows how PSMMR tends to underpredict in moist areas. The QITCZ case of underprediction is more complicated than the STH case. Underprediction could be a result of the ECMWF analysis of 3.4 cm and the OLR observation of 240 W m^{-2}. If the ECMWF was a more representative QITCZ value of 4.2 cm and OLR was 200 W m^{-2} the PSMMR would be 50.7 kg m^{-2}. This is a more accurate value, but still an underprediction of SMMR by 4.3 kg m^{-2}. The systematic biases in PSMMR might be improved by using different regression equations in different features, but the current data set is too small for such a procedure.

The plot of SMMR vs. PSMMR is shown in Fig. 15. There are biases in the PSMMR, but there are no extreme outliers as on the left side of the SMMR vs. ECMWF plot. The systematic biases in PSMMR are an underprediction in moist areas and an over prediction in dry areas. The largest underpredictions occurred within the AITCZ (typically 15 kg m^{-2}); the largest overpredictions occurred within the TP and EDZ (typically 10 kg m^{-2}).

When the data are stratified by feature to examine how well SMMR could be predicted within features there are no statistically significant parameters or coefficients of determination. The mean values and standard deviations for PSMMR are in Table 5. PSMMR means are similar to the SMMR values and there are no
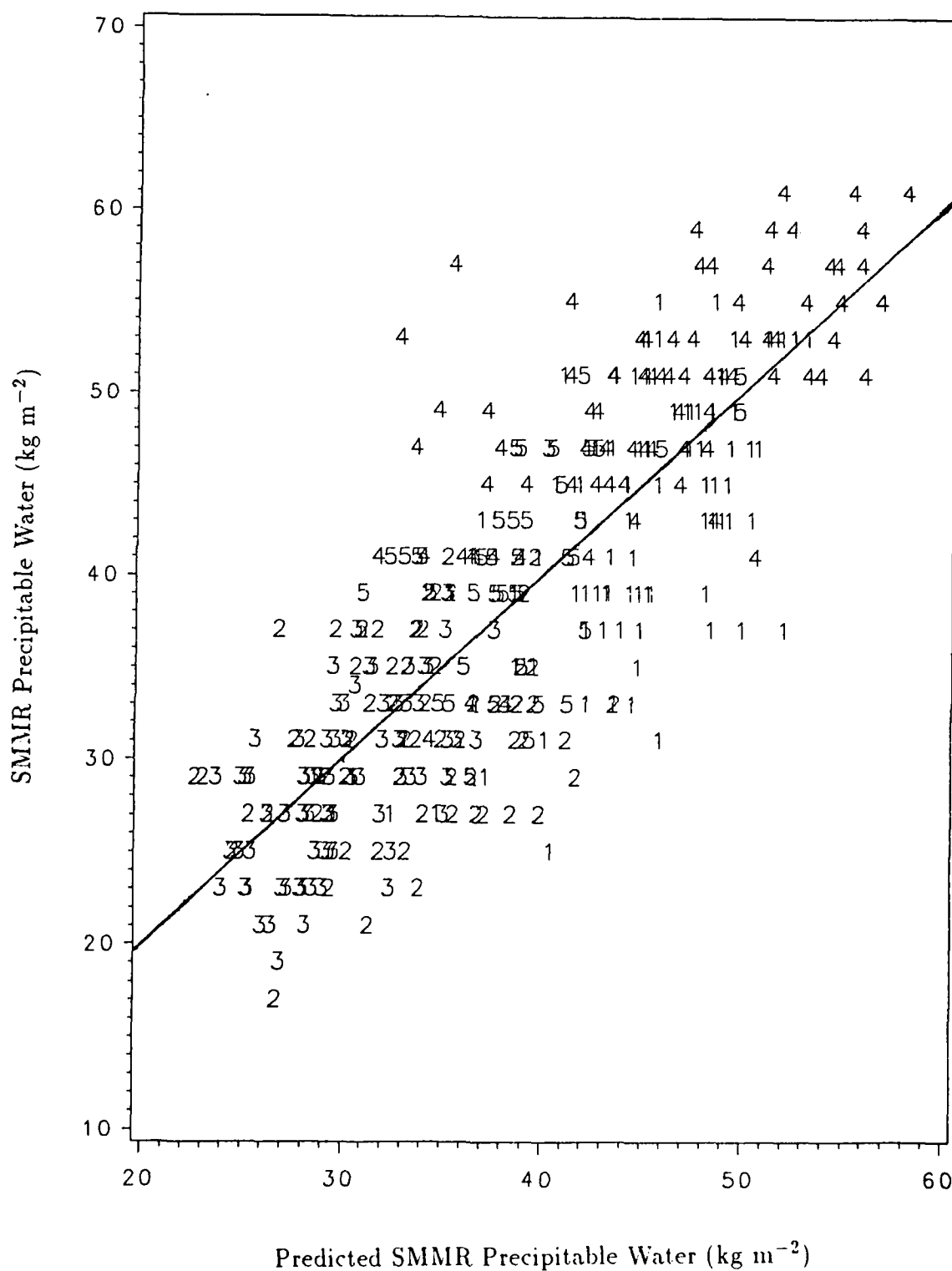
Figure 15. Plot of SMMR vs. PSMMR. The straight line would be a perfect fit. The numbers represent observations within individual synoptic features: 1=TP, 2=EDZ, 3=STH, 4=AITCZ, 5=QITCZ.

Table 5.   Mean values for SMMR and PSMMR and standard deviations of PSMMR stratified by synoptic feature. Mean value units are (kg m^{-2}).

	SMMR Mean	PSMMR Mean	PSMMR Standard Deviation
TP	42.1	44.3	5.7
EDZ	31.9	33.4	4.6
STH	28.1	29.9	3.7
AITCZ	49.4	45.5	6.6
QITCZ	41.0	38.7	4.0

systematic variations in the means. The standard deviations of the PSMMR values are all smaller than the observed SMMR standard deviations.

A SMMR swath shown in Fig. 16 was chosen to demonstrate the capabilities of the model. The swath was chosen because of the variety of features sensed. Within the swath (from north to south) are the STH, TP, ITCZ, equatorial clear area (ECA), and area of convection (CONV) in the southern hemisphere. The precipitable water content of the swath was computed using six different models that progressively added more and different combinations of TOVS 11, TOVS 12, OLR and the ECMWF analysis.

The ECMWF and OLR model increased the precipitable water content above the ECMWF analysis along the entire swath. The increase was about 10 kg m^{-2} in the partly cloudy STH, but only small increases were noted along the rest of the swath. An increase of about 6 kg m^{-2} occurred in the equatorial clear area and could be attributed to the processing techniques used to smooth and grid the OLR data.
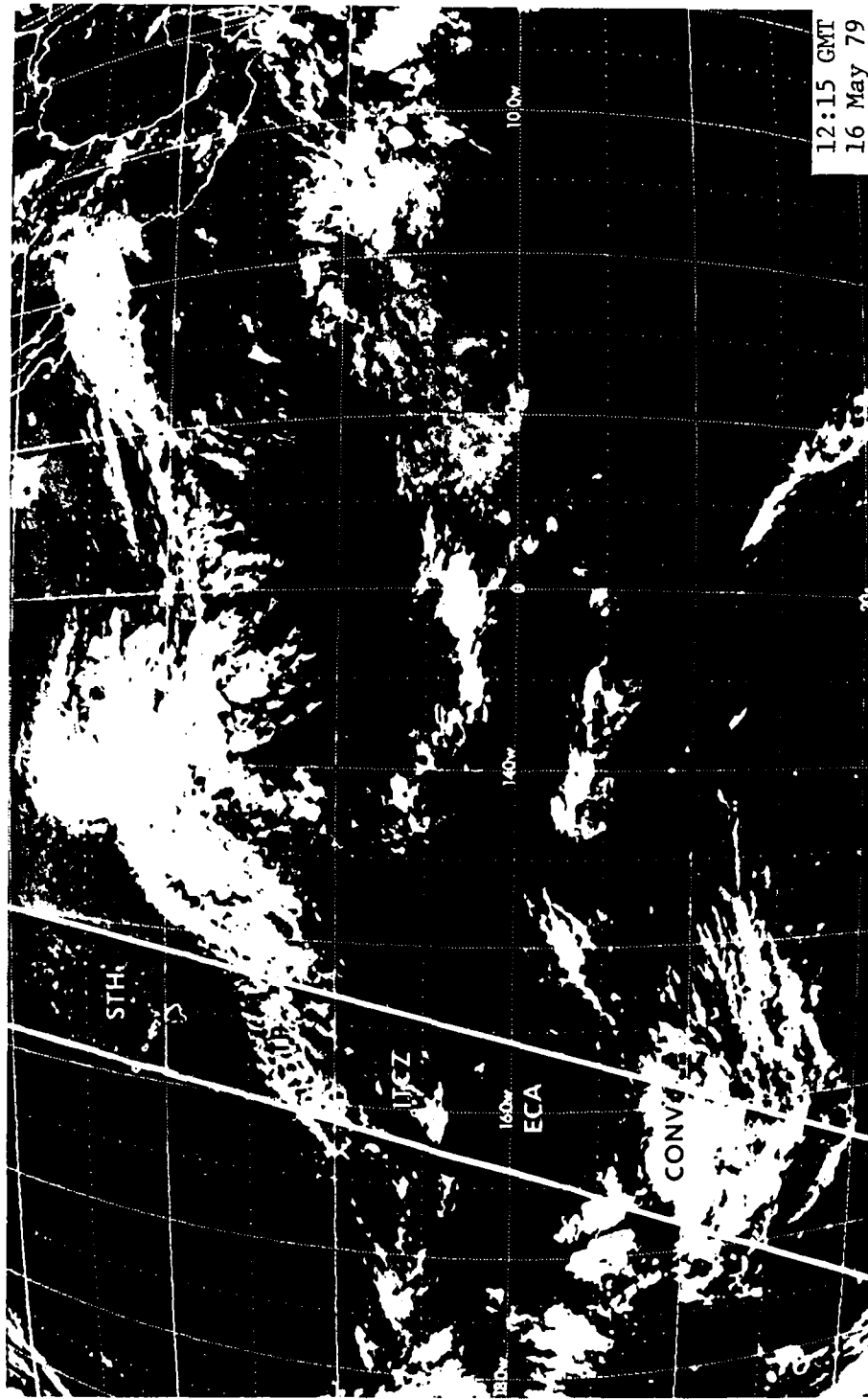
Figure 16.   GOES West IR image for May 16, 1979 at 1200 GMT. The SMMR swath is contained within the two white lines. Features are marked STH, TP, ITCZ, ECA and CONV.

Combining ECMWF with either TOVS 11 or TOVS 12 provided similar results in most areas, as would be expected from the high TOVS 11 vs. TOVS 12 correlation. In the equatorial clear area TOVS 11 did provide a 4 kg m^{-2} better increase in the precipitable water content than the TOVS 12. Differences in the TOVS channels in a clear column area can indicate where the moisture is located. In this example most of the moisture would be located lower in the atmosphere and detected better by TOVS 11.

The three best three variable models were compared, but the improvements over the two variable models were small. Differences between the three variable models were also small.

The models' problems in predicting the moisture in the STH probably result from the presence of moisture evident on the original satellite image as low clouds between 20 and 30 °N. All of the models provided a good estimate in the TP, ITCZ and convective area in the southern hemisphere. In the equatorial clear area the TOVS 11 and TOVS 12 provided a 50% increase in the moisture, but the ECMWF analysis was initially too low. The ability to predict SMMR seems to depend on the synoptic situation and the type of data used.

Three dimensional plots of data are prepared to examine the variations in patterns that are detected by SMMR, ECMWF and PSMMR. The plot of SMMR in

Fig. 17 is from May 16, 1979 at 1200 GMT. The vertical axis has SMMR precipitable water estimates, the latitude axis is north to south along the length of the SMMR swath (with the subsatellite point at 3.5° across swath) and the degrees across the SMMR swath axis depicts the variation across the 7° SMMR swath. The plot of 45° latitude verse degrees across the SMMR swath tends to stretch the figure meridional since the SMMR swath is only 7° wide, but there is not much zonal variation across the narrow SMMR swath. Indicated on the plot are the position of the STH, TP, ITCZ, ECA and CONV. The three dimensional plot reveals the meridional variation in the precipitable water field estimated by SMMR.

The plot of ECMWF precipitable water in Fig. 18 is from ECMWF estimates that are collocated with SMMR observations from May 16, 1979 at 1200 GMT. The vertical axis has ECMWF precipitable water estimates with the other markings the same as in Fig. 17. The ECMWF analysis is the most important contribution to the prediction of SMMR and is a representative analysis of the moisture field in all areas except the ECA.

The plot of PSMMR estimated precipitable water in Fig. 19 is computed from collocated data on May 16, 1979 at 1200 GMT using equation 3. The vertical axis is PSMMR precipitable with the other markings the same as in Fig. 17. The comparison of PSMMR will be accomplished by studying data along the western edge of the SMMR swath.

Figure 20 compares ECMWF, SMMR, and PSMMR values. The data are taken from the western edge of the SMMR swath depicted on horizontal axis is from 30°N
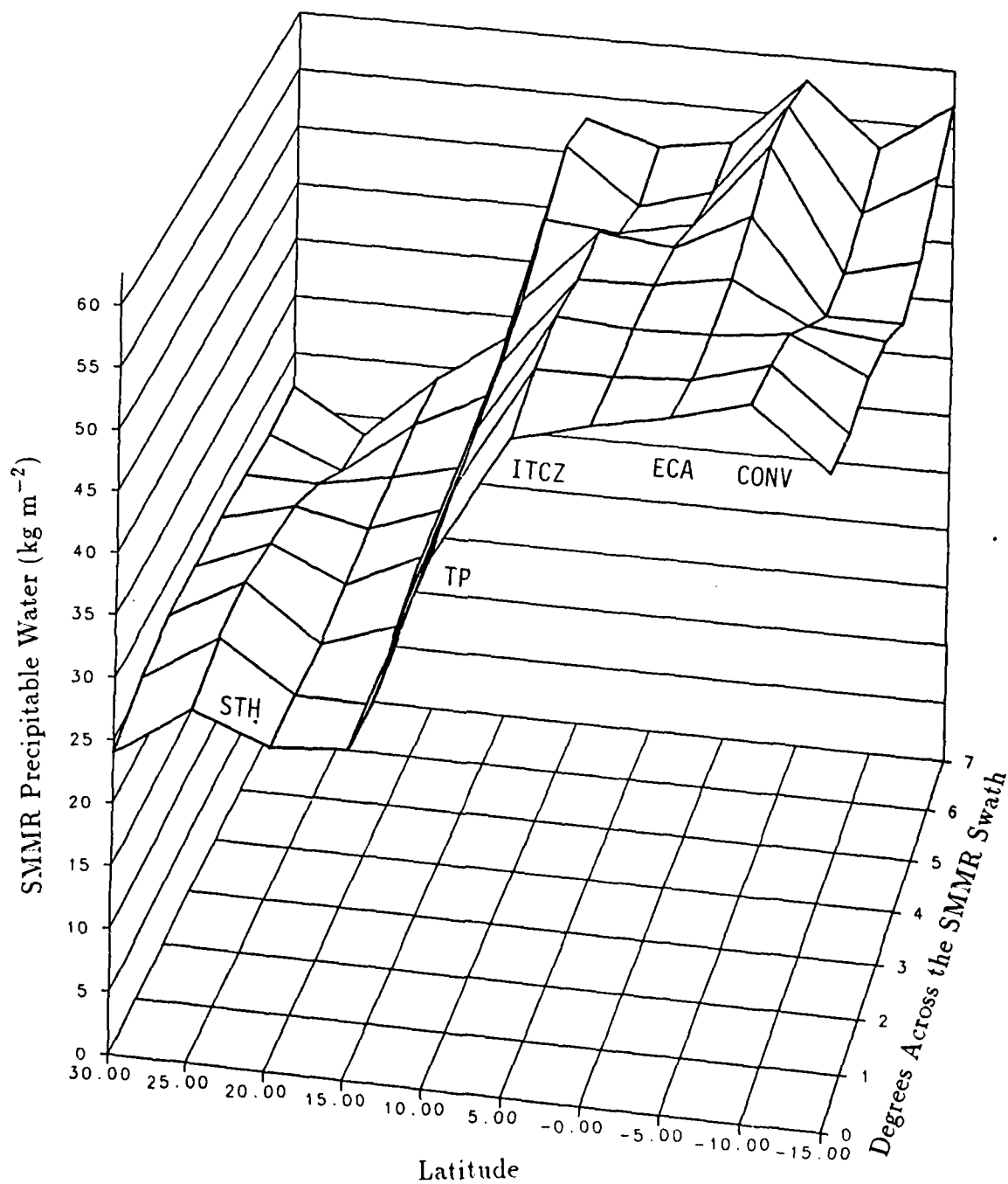
Figure 17. Plot of SMMR for May 16, 1979 1200 GMT. Positive latitude values are north and negative values are south. See text for labels.
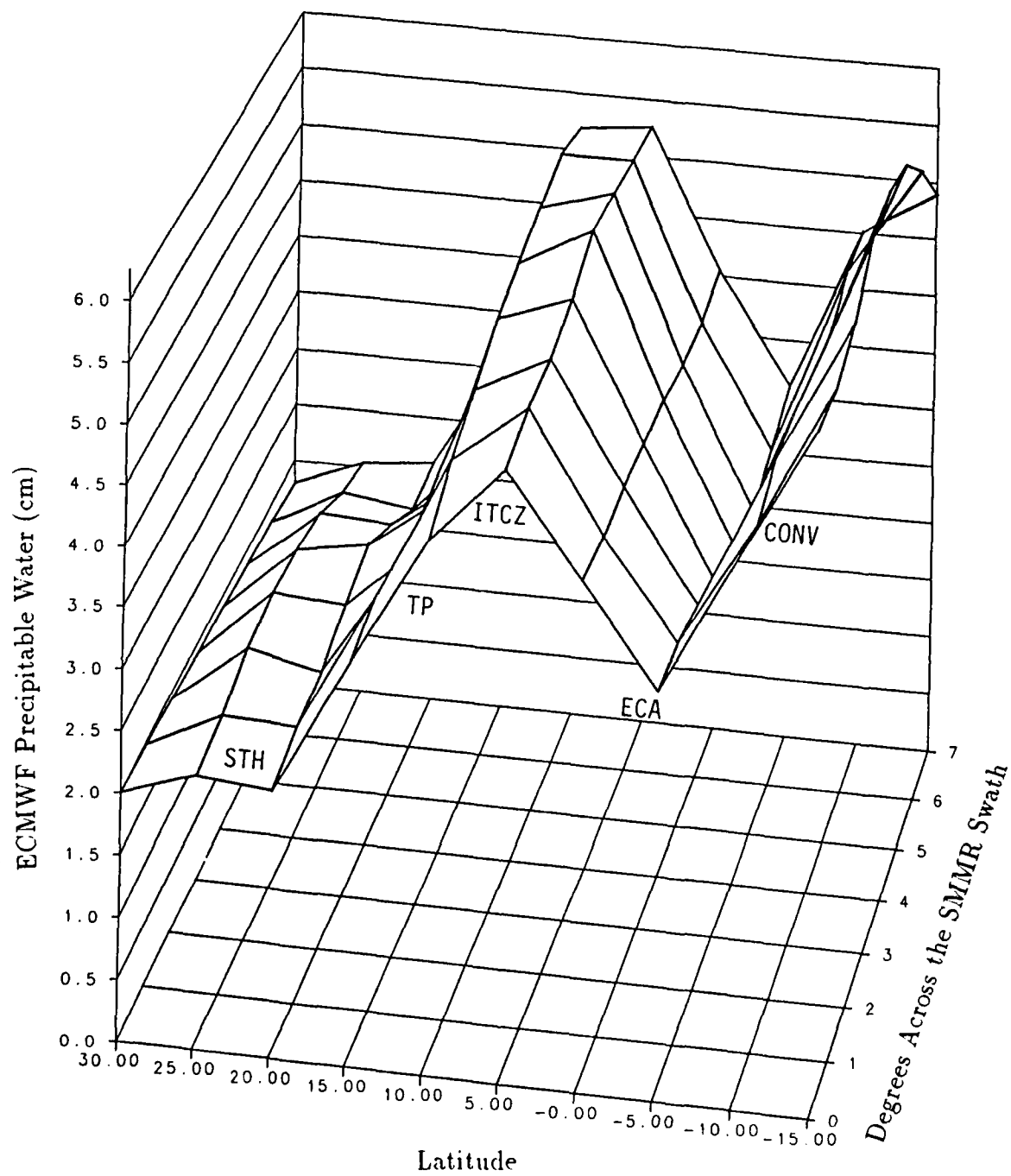
Figure 18.   Plot of ECMWF for May 16, 1979 1200 GMT. Positive latitude values are north and negative values are south. See text for labels.
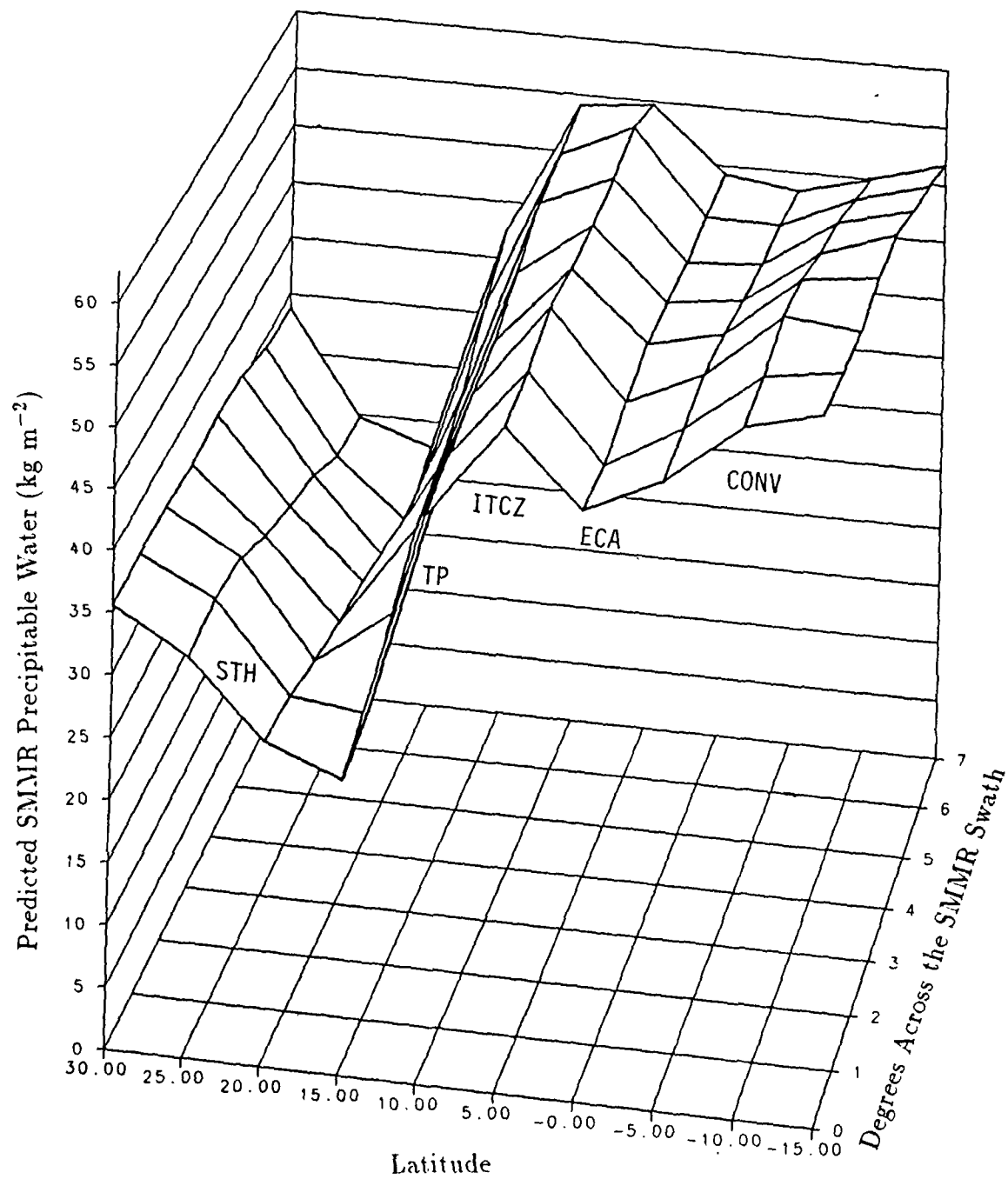
Figure 19.   Plot of PSMMR for May 16, 1979 1200 GMT. Positive latitude values are north and negative values are south. See text for labels.
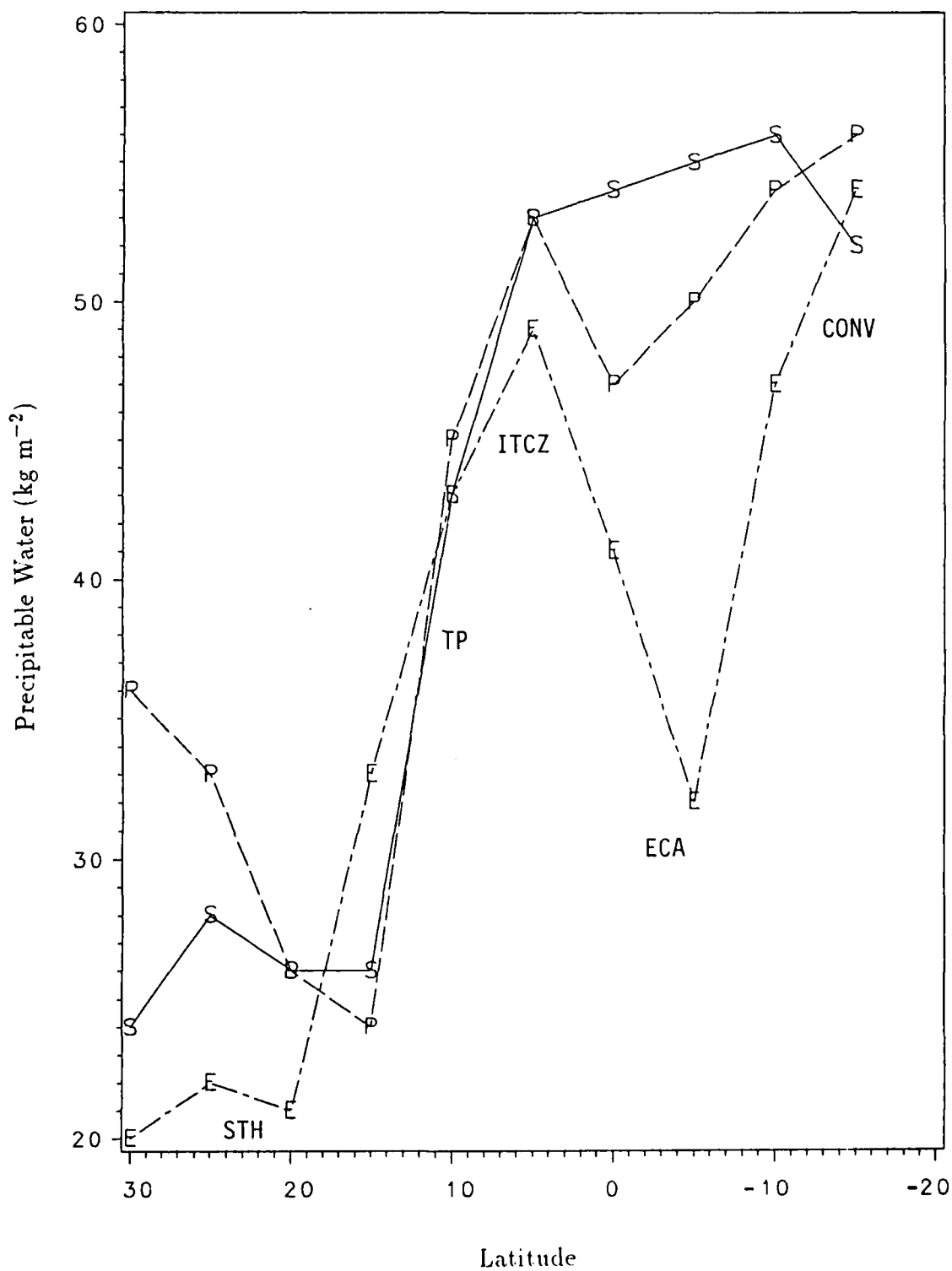
Figure 20. Plot of SMMR, PSMMR, and ECMWF. For 1200 GMT May 16, 1979 along the western edge of the SMMR swath. Data points P=PSMMR, S=SMMR and E=ECMWF. See text for labels.

to 15°S. The vertical axis has precipitable water data with the ECMWF data are converted to units of kg m^{-2}. The ECMWF estimates two maxima at 3° N (ITCZ) and 7° S (CONV). SMMR in Fig. 20 has a similar pattern except from 5° S to 15° S the precipitable water content is consistently high through the region designated ECA. The PSMMR corrects for this area based on the TOVS and OLR infrared observations from 5° S to 15° S. Unfortunately the PSMMR increases the precipitable water in the STH about 34% at 30° N in Fig. 20. The errors in estimating the precipitable water field are a combination of overall systematic biases and data problems in areas where clear column radiances are not available. The ability of SMMR to detect the synoptic scale moisture has been demonstrated. TOVS 11, TOVS 12, OLR, and the ECMWF analysis individually are not exceptional moisture estimators, but combining them results in improvements to the precipitable water quantities and moisture field.

In summary the mean precipitable water content of five tropical synoptic features are quantified from SMMR data and the SMMR data confirmed that the STH is dryer than the EDZ. Examination of the ITCZ has shown areas where high convective cloud tops are absent still may have a high precipitable water content. Correlations between SMMR, TOVS 11, TOVS 12, OLR and the ECMWF analysis show there are usable relationships between the data and between TOVS 11, TOVS 12, OLR, the ECMWF analysis and SMMR precipitable water estimates. The best correlation to SMMR precipitable water was with the ECMWF analysis and worst was with TOVS 12. When the data are stratified by synoptic feature the correlations between the data are reduced and not meaningful for much of the data. Plots of the data show the scatter present and how a specific value in one observation

type span almost the entire range in another. Correlations with other types show that OLR data are unreliable as an indicator of atmospheric precipitable water. All five water vapor estimates are correlated; unfortunately most of the correlation is explained by regional differences and not by synoptic structure within individual systems. Prediction of SMMR demonstrated that 67% of SMMR variance can be predicted from combining model analysis and satellite observations. The PSMMR can differentiate between synoptic scale features, but is not able to determine the structure within features. Prediction of SMMR demonstrated that improvements can be made to moisture estimation by combining different types of data, but the type of data and the synoptic situation are important considerations.

CHAPTER VI

RAINFALL

Rainfall was computed from algorithms used by Katsaros and Lewis (1986) and Warner (1984) to investigate differences between algorithms and the TP and AITCZ rainrates (these were the only features with precipitation). The data are stratified by feature and month to investigate differences in area and intensity of the rainfall.

The algorithm used by Katsaros and Lewis (1986) is experimental and optimized for use in the area off the Pacific coast of Washington. Applying the algorithm to the tropical rain systems resulted in a 30% increase in area covered by light rain, compared to Warner's method, and limitation of the highest rain values to 6 mm h^{-1}. This algorithm was not used any further due to these characteristics.

The algorithm used by Warner (1984) was tested in a tropical monsoon and found to have comparable area coverage to an airborne radar. The highest rainrates detected in the monsoon from SMMR were 18 mm h^{-1}. The rainrate estimates from SMMR corresponded well with areas of cold cloud tops on the GOES IR imagery. The cold cloud tops are an indication of rainfall on IR images. The actual rainfall intensities are difficult to analyze due to the lack of a "ground truth"; therefore only relative rainrate differences between features are investigated.

Rain events detected by SMMR during the period of this study are identified as being associated with the TP or AITCZ. The TP rain events are distinctly different from those within the AITCZ. AITCZ rain events were all found south of 7°N and the TP rain events were all found north of 10°N. Using OLR data, Hayes (1988) found a similar situation where the ITCZ tended to be closer to the equator when considerable active convection was present. There was some difficulty in distinguishing the TP rain events from midlatitude rain events, so in conjunction with the latitudinal restriction TP rain must be a part of or have previously been a part of a TP.

VI.1 Behavior of TP and AITCZ Rainfall

Table 6 shows the SMMR orbit number, feature, day/night, and number of 60 km rain pixels detected within each rainrate intensity. The table is arranged as histogram, with TP rain events on top and AITCZ rain events on bottom displayed in order of decreasing intensity. The overall pattern indicates an equality of rainrate distributions within the TP and AITCZ. While rainrates are indicated in Table 6 area averages are an important feature of SMMR data. SMMR will not indicate the highest intensity present within a pixel, but the rainrate will indicate relative intensity between pixels. Some biases are in the rain data due to the method of sampling. The biases result from meridionally oriented SMMR orbits being used to sample TPs, that are meridionally oriented, and the ITCZ, which is zonally oriented.

Table 6. Rainfall events detected by SMMR. The events are separated by feature TP and ITCZ (IT), day (D), night (N), and rainrate intensity ($R1 = 1$ mm h^{-1} etc.). Rainrate values indicate the number of 60 km pixels detecting rain. Orbit numbers (orbit) from 1191-1363 were in January and 2793-2857 were in May 1979.

OBS	ORBIT	FEATURE	DN	R1	R2	R3	R4	R5	R6	R7	R8	R9	R10	R11	R12	R13	R14	R15	R16
1	1253	TP	D	28	17	12	2	10	5	7	7	2	5	7	5	1	2	1	3
2	1363	TP	D	20	11	9	9	4	2	8	9	1	0	0	1	0	0	1	
3	1273	TP	N	60	15	7	12	5	7	7	3	6	2	0	3	0	1		
4	1217	TP	N	35	7	2	2	4	2	0	2	2	2	1	0	1	1		
5	1197	TP	D	70	42	24	7	5	2	9	7	5	8	4	1				
6	1280	TP	D	33	16	5	9	3	1	6	6	1	2	0	1				
7	1300	TP	N	21	11	4	3	2	2	1	4	1	2	2					
8	2857	TP	D	36	7	3	4	1	1	2	3	0	1						
9	1335	TP	D	38	13	6	3	1	1	1	1	1							
10	1225	TP	D	10	3	4	2	0	0	0	1								
11	2855	TP	N	7	3	1	1	0	0	1									
12	1328	TP	D	13	4	4	1	2	0	2									
13	2801	TP	D	11	5	1													
14	1307	TP	D	31	4														
15	2829	TP	D	2	1														
16	1218	IT	N	25	5	8	1	6	2	3	1	0	1	0	0	0	0	0	1
17	1336	IT	D	9	10	4	3	4	2	3	1	1	1	1	0	1			
18	1191	IT	N	46	22	9	5	13	5	0	3	2	0	1	1				
19	1246	IT	N	28	17	8	9	9	9	6	3	2	0	1					
20	2802	IT	D	10	7	0	1	3	2	5	5	0	1						
21	1301	IT	N	25	6	4	2	2	0	0	0	1							
22	1254	IT	D	15	6	4	8	3	6	3	2								
23	2793	IT	N	13	4	4	6	1											
24	1309	IT	D	15	9	2	2	1											
25	2794	IT	N	22	5	11	5												
26	2822	IT	N	15	6	3	1												
27	2800	IT	D	8	1	3	1												
28	1274	IT	N	7	1	1	2												
29	2828	IT	D	7		0													
30	2821	IT	N	3															
31	1245	IT	N	2															

Table 7. Percentage occurrence of rainrates within TPs, AITCZ and All rain events
combined. TP and AITCZ percentages are the percentage of the total
number of pixels for each rainrate within the features. All rain events
combine the TP and AITCZ rainrates and are the percentage of the total
number of pixels for each rainrate. "X" indicates no data available.

Rainrate mm h^{-1}	1	2	3	4
TP	44.2	16.9	8.5	5.8
AITCZ	43.3	17.9	10.4	8.0
All Observations	43.8	17.3	9.4	6.7

Rainrate mm h^{-1}	5	6	7	8
TP	3.9	2.5	4.7	4.7
AITCZ	7.3	4.5	3.5	2.6
All Observations	5.2	3.2	4.2	3.8

Rainrate mm h^{-1}	9	10	11	12
TP	2.0	2.3	1.5	1.3
AITCZ	1.0	0.5	0.5	0.2
All Observations	1.8	1.7	1.1	0.8

Rainrate mm h^{-1}	13	14	15	16
TP	0.2	0.4	0.2	0.3
AITCZ	0.2	X	X	0.2
All Observations	0.2	0.3	0.1	0.3

The data are evenly divided with 16 ITCZ and 15 TP events, and 17 day and

14 night events. The percentage of pixels indicating rain out of the total number

of pixels in each rainrate is shown in Table 7. TP and AITCZ percentages are the

percentage of the total number of pixels for each rainrate within the features. All

percentages combine the TP and AITCZ rainrates and are the percentage of the total

number of pixels for each rainrate. The per cent of pixels in each rainrate category

is statistically identical for the TP and AITCZ. This would imply that both the TPs

and AITCZ in this study are tropical convective type rain systems, since the AITCZ

is a convective rain system. The day/night percentages of pixels in each rainrate are also statistically identical indicating minimal diurnal cycle.

The absence of a diurnal cycle in SMMR rain data does not imply that no diurnal cycle exists in rain from this area. Meisner and Arkin (1987) used three-hourly GOES IR data from December 1981 thru November 1984, from 50°N to 50°S, 175°E to 25°W to analyze rainfall cycles. Over the Pacific ocean they found diurnal rainfall cycles in the convergence zones that were characterized by a near-noontime maximum. Albright et al. (1985) used GOES IR data from 0000, 0600, 1200 and 1800 GMT from January 1 to February 28, 1979 in an area from 20°N to 20°S and 170°E to 130°W to study the diurnal cycle of rainfall. They divided the region into five subregions, two of which were the AITCZ and TP. They used percentage deviation from the daily mean of cloud tops colder than −36°C, which has been previously related to rainfall, to study the diurnal variation in rainfall. In the AITCZ they found a +10% deviation at noon local and a −10% deviation at midnight local in the cold cloud tops. In the TP region there was a −10% deviation at noon local and a +15% deviation at midnight local in the cold cloud tops. Combining these effects of area and time would tend to remove the diurnal variation of rainfall from the midnight local and noon local SMMR data in the area of this study.

Stratifying the rain events into January and May shows differences in the rainfall between two types of TPs. As observed on satellite images the January TPs tend to be larger, longer lasting and occur more frequently than the May TPs. During the ten data days there were 31 rain events detected by SMMR that could be classified as either TP or AITCZ rain events. The 20 January events had a

total of 1261 pixels of rain and had a peak rainrate of 16 mm h^{-1} four times. The 11 May events had 254 total pixels of rain and had a peak rainrate of 10 mm h^{-1} two times. Combining GOES IR image and SMMR information results in a analysis that the January TPs had about twice the rain intensity as the May TP.

VI.2   TP Rainfall Spatial Distribution

Of the 18 SMMR passes over TPs, 15 detected rain and these rain events were spread along the entire length of the TP. Analysis of which areas in TPs were raining found that four of seven SMMR passes over the northern half of TPs had rain events while all passes over the southern half of the TP had rain. This might indicate that the southern half of TPs are associated with the AITCZ, while the northern half of TPs are mostly rain free clouds with only scattered rain cells. The rain was not organized in any particular pattern in any part of the TP. The location and disorganization of TP rain might imply the rain is tropical.

Use of SMMR in the investigation of rainfall has shown that significant areas of TPs are raining and the distribution of rain is similar to the AITCZ. Diurnal differences in the noon and midnight local SMMR overpass times are insignificant. The different rainrate algorithms have different areas of coverage and intensities that need to be adapted to the type of rainfall they will sample.

VI.3   TP Area Averaged Rainfall Estimates

Area averaged estimates of the rainfall in TPs are estimated through analysis of the percentage of rain coverage. First the cloud shield of a TP was defined, as by

McGuirk and Thompson (1984), as a continuous band of upper and midlevel clouds at least 2000 km in length that originated from a cloud source equatorward of 15°N and extending poleward of 15°N. Then the area of the TP upper and midlevel cloud shield was defined by estimating a TP length and width. The southwest end of the TP axis was defined as the center of the cloud shield at the narrowest point north of 7°N and the northeast end of the axis was defined as the first occurrence of a distinct break, narrowing or when the coast of North America was reached. The northeast end of the axis was the most difficult to define and subject to some interpretation. Finally the area coverage of rainfall was estimated using GOES IR images, SMMR rainrate estimates and extrapolation of SMMR rain areas to clouds that appeared similar on the GOES IR images. Twenty GOES IR images corresponding to the local midnight and noon SMMR overpass times were examined.

Estimates of rain coverage shown in Table 8 range from 30% to 5% (in increments of 5%) of the entire TP cloud shield raining. The accuracy of these estimates is thought to be within a factor of 2. Of the 20 TP samples only two had 30% coverage, one had 20% coverage, ten had 10% coverage and seven had 5% area coverage of rain. Separating the TPs into January and May cases shows that no May cases had larger than 10% coverage of rain indicating the January cases are stronger than the May cases.

In summary the results of the SMMR rain data are difficult to quantify, but they do indicate a few things. SMMR rain algorithms need to be developed for different types of rain. The TP and AITCZ rainrates in the study are statistically identical and

Table 8. Percentage of the TP cloud shield raining for twenty TPs. Dates of the SMMR times are indicated for the midnight (Mid) and noon local SMMR overpass times. Length of the TP axis, average width and Percentage of the cloud shield raining are also indicated.

Date	Time	Length (km)	Width (km)	Percentage
18 Jan	Mid	2400	1700	30
	Noon	2800	1500	20
20 Jan	Mid	2300	700	10
	Noon	2200	500	5
22 Jan	Mid	2200	1200	10
	Noon	2600	1400	10
24 Jan	Mid	2700	1300	30
	Noon	2500	900	10
26 Jan	Mid	2500	500	10
	Noon	2500	500	10
28 Jan	Mid	2100	700	5
	Noon	2200	700	5
30 Jan	Mid	2800	1300	10
	Noon	2700	1000	10
14 May	Mid	2300	500	5
	Noon	2700	600	5
16 May	Mid	3400	600	5
	Noon	3800	500	5
18 May	Mid	2800	1100	10
	Noon	2300	700	10

could indicate that rainfall in both of these features are convective, since the AITCZ rain is known to be convective. The January TPs studied have greater intensities and area coverage of rain than the May TPs.

CHAPTER VII

SUMMARY AND DISCUSSION

Nimbus-7 SMMR data from January and May 1979 were examined to quantify typical moisture structure of tropical Pacific Ocean features. Data were collected from collocated observations of SMMR, TOVS 11, TOVS 12, OLR, and the ECMWF analysis to determine their relationship and capability to estimate and predict precipitable water. A multiple linear regression equation was developed that would predict precipitable water as estimated from SMMR using ECMWF, TOVS 11, TOVS 12, and OLR; these estimators are listed in decreasing order of importance in the regression equation.

A rainfall analysis of the TP and ITCZ was accomplished by processing SMMR data using an algorithm developed by Lipes (1981) and Katsaros and Lewis (1986). The spatial coverage and intensities of the two algorithms were investigated within the context of the two features.

The main results of the study may be summarized as follows. SMMR precipitable water estimates provide detailed information on the moisture structure in all areas of the tropics except in areas of heavy precipitation. SMMR was able to quantify the mean precipitable water content and standard deviation of the TP, STH, EDZ, AITCZ and QITCZ. Through identification of the characteristic moisture content of each feature and SMMR precipitable water estimates revealed that the TP and QITCZ have a similar moisture content, but the TP has a larger standard deviation.

SMMR, TOVS 11, TOVS 12, OLR and the ECMWF analysis are all correlated; unfortunately most of the correlation is explained by regional differences, not by synoptic structure.

In the prediction of precipitable water using SMMR as a "ground truth", most of the SMMR variance can be predicted from TOVS 11, TOVS 12, OLR and the ECMWF analysis observations. The model explained 67% of the variance in SMMR data and the ECMWF analysis alone explained 55% of the variance. The model predictions can differentiate between synoptic features, but can not determine synoptic structure within a feature.

SMMR rainrate data can define characteristics of spatial coverage and relative rainrates of tropical rain features. The per cent frequency of rainrate categories within TPs and ITCZ are identical, implying the rain studied was the same type of tropical convection. There were no variations in spatial coverage or rainrates for the SMMR overpass times of noon and midnight. The percentage of a TP covered by rain in this study varied from 30% to 5% with the January TPs having a greater area of rain than the the May TP.

The objective of this research was accomplished. The moisture content of tropical Pacific Ocean synoptic features was quantified, the capabilities of the satellite data were examined, precipitable water fields were predicted, and precipitation within TPs and the AITCZ were compared. It was also found that TOVS, OLR and ECMWF analysis data are able to determine the synoptic structure of moisture and precipitation, but are not able currently to resolve details below the synoptic scale.

REFERENCES

Albright, M.D., E.E. Recker, R.J. Reed, and R. Dang, 1985: The diurnal variation of deep convection and inferred precipitation in the central tropical pacific during January–February 1979. *Mon. Wea. Rev.*, **113**, 1663–1680.

Anderson, L.L., 1986: Multispectral analysis of a tropical radiance set from the TIROS operational vertical sounder. PhD Dissertation, Dept. of Meteorology, Texas A&M University, College Station, TX, 77843, 229 pp.

Beauchamp, J.G., 1988: The impact of sun glint on the SMMR radiances. Report, NASA/Goddard. Greenbelt, MD, 19 pp.

Blackwell, K.G., 1987: Synoptic scale sensitivity of TIROS-N moisture channels in the tropics. M.S. Thesis, Dept. of Meteorology, Texas A&M University, College Station, TX, 77843, 124 pp.

Cadet, D.L., 1983: Mean fields of precipitable water over the Indian Ocean during the 1979 summer momsoom from TIROS-N soundings and FFGGE data. *Tellus*. **35B**, 329–345.

Fu, C.C., and N.S. Chung, 1988: Abnormal calibration data from the Nimbus-7 SMMR and its impact on the retrieved brightness temperatures and geophysical parameters. report, NASA/Goddard, Greenbelt, MD, 59 pp.

Gloersen, P., et al., 1984: A summary of results from the first Nimbus-7 SMMR observations. *J. Geophys. Res.*, **89**, 5335–5344.

——, 1987: In orbit calibration adjustment of the Nimbus-7 SMMR. Report, NASA No. 100678, NASA/Goddard, Greenbelt, MD, 39 pp.

Hayes, P.M., 1988: Active modes of the Pacific ITCZ. M.S. Thesis, Dept. of Meteorology, Texas A&M University, College Station, TX, 77843, 90 pp.

Katsaros, K.A., and R.M. Lewis, 1986: Mesoscale and synoptic scale features of north pacific weather systems observed with the scanning multichannel microwave radiometer on NIMBUS-7. *J. Geophys. Res.*, **91**, 2321–2330.

Kim, S.T., D. Han, and H.D. Chang, 1984: Analysis and correction of the brightness temperature measured in the 21GHz horizontal channel of the Nimbus-7 scanning multichannel microwave radiometer. Report, NASA No. SASC-T-5-5100-0004-0026-84. NASA/Goddard. Greenbelt, MD, 51 pp.

Lipes, R., 1981: SMMR mini-workshop IV. Report, Publ. 622-634, Jet Propulsion Laboratory, Pasadena, CA, 135 pp.

Meisner, B.N. and P.A. Arkin, 1987: Spatial and annual variations in the diurnal cycle of large-scale tropical convective cloudiness and precipitation. *Mon. Wea. Rev.*, **115**, 2009-2031.

McGuirk, J.P., and A.H. Thompson, 1984: Transient tropical disturbances within the pacific hadley cell. *Proc. 15th Tech. Conf. on Hurricanes and Tropical Meteorology*, Miami, Amer. Meteor. Soc., 249-255.

——, ——, and N.R. Smith, 1987: Moisture bursts over the tropical Pacific Ocean. *Mon. Wea. Rev.*, **115**, 787-798.

——, ——, and L.L. Anderson, Jr., 1989: Synoptic scale moisture variation over the tropical Pacific Ocean. *Mon. Wea. Rev.*, *(accepted for publication)*.

Prabhakara, C., H.D. Chang, and A.T.C. Chang, 1982: Remote sensing of precipitable water over the oceans from NIMBUS-7 microwave measurements. *J. of Appl. Meteor.*, **21**, 59-68.

Schaefer, J.R., 1985: Observing the synoptic structure of two moisture bursts. M.S. Thesis, Dept. of Meteorology. Texas A&M University, College Station, TX, 77843, 145 pp.

Smith, W.L., H.M. Woolf, C. Hayden, D. Wark, and L.M. McMillin, 1979: The TIROS-N operational vertical sounder. *Bull. Amer. Meteor. Soc.*, **58**, 1177-1187.

Spencer, R.W., 1986: A satellite passive 37 GHz scattering-based method for measuring oceanic rain rates. *J. Climate Appl. Meteor.*, **25**, 754-766.

Stockton J.R., 1986: The structure of a late-spring moisture burst. M.S. Thesis, Dept. of Meteorology, Texas A&M University, College Station, TX, 77843, 90 pp.

Systems and Applied Sciences Corporation, 1985a: User's guide for the Nimbus-7 scanning multichannel microwave radiometer (SMMR) CELL-ALL tape. Report, NASA No. SASC-T-5-5100-0004-011-84, NASA/Goddard, Greenbelt, MD, 62 pp.

_____, 1985b: User's guide for the Nimbus-7 scanning multichannel microwave radiometer (SMMR) PARM tapes year 1, 2 and 4. Report, NASA No. SASC-T-5100-0004-016-84, NASA/Goddard, Greenbelt, MD, 87 pp.

Warner C., 1984: Satellite observations of a monsoon depression. Report, NASA No. NAG 5-297, 98 pp.

Wilheit, T.T.,and A.T.C. Chang, 1980: An algorithm for retrieval of ocean surface and atmospheric parameters from the observations of the scanning multichannel microwave radiometer. *Radio Science*, **15**, 525–544.

VITA

Jeffrey David Fink was███.
He is the second of three children born to ███████████████████████████ After
attending many schools around the United States and in England he graduated from
MacArthur High School San Antonio, Texas in 1975.

Jeffrey attended Texas A&M University from 1975 to 1979, participating in the
Corps of Cadets and Air Force ROTC. He graduated in May 1979 with a B.S. in
Meteorology and was commissioned a 2nd Lieutenant in the United States Air Force.

After entering active duty in September 1979 he attended Undergraduate Pilot
Training Training at Reese AFB, Texas. In October 1980 he was assigned to fly
the C-130 Hercules at Little Rock AFB, Arkansas. In July 1984 he was assigned
to Yokota AB, Japan where he flew as an instructor pilot and standardization and
evaluation pilot. He was selected for an AFIT advanced degree at Texas A&M and
in July 1987 departed Japan.

Jeffrey is married to the former ██
███████████████████████████.

██

████████████████████████████████